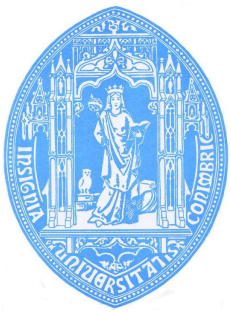

Novel approach to vascular network modeling in 3D

Maria Margarida Dias Soares Quinas Guerra

Project oriented by Professor Rui Travasso

Center for Computational Physics

Thesis submitted to the
Faculty of Science and Technology
In partial fulfillment of the requirements
For the MSc degree in Biomedical Engineering

Curricular Unit of Project
Faculty of Science and Technology
University of Coimbra

'Science is a great game.
It is inspiring and refreshing.
The playing field is the universe itself.'

Isidor Isaac Rabi (1898-1988)
U. S. physicist
Nobel prize 1944

Resumo

A angiogénese, o processo através do qual novos vasos sanguíneos crescem a partir da vasculatura pré-existente, é um dos processos centrais subjacentes às redes vasculares. Está implicada em mais de 70 doenças até agora, tendo-se tornado no objecto de estudo de muitos investigadores, no campo da investigação biológica mas também na área computacional. Sendo que é crucial para o desenvolvimento de cancros na sua fase vascular, muitos investigadores têm dedicado os últimos 15 anos ao seu estudo, que envolve uma grande quantidade de diferentes factores, na procura de terapêuticas que eventualmente tenham a angiogénese como alvo.

A angiogénese é um processo biológico complexo. Neste trabalho começa-se por revêr alguns dos principais mecanismos essenciais para a angiogénese.

Vários modelos matemáticos que modelam a angiogénese combinados com simulações computacionais têm sido propostos nos últimos 30 anos, alguns em duas dimensões, os mais recentes em 3D, e considerado vários aspectos diferentes envolvendo a angiogénese: quimiotaxia, haptotaxia, angiopoietinas e propriedades da Matriz Extracelular.

Esta tese envolve a simulação de um modelo híbrido multi-escalar de fases que descreve a dinâmica da interface entre os novos capilares e o estroma. Quatro equações modelam o comportamento das células endoteliais proliferativas em resposta a um gradiente de factores pró-angiogénicos (T), conduzindo a um crescimento e evolução temporal de uma árvore de vasos sanguíneos a partir de rebentos que brotam do capilar inicial. Estes novos rebentos são puxados por células de ponta activas como resultado de processos internos regulatórios, e movem-se com uma velocidade proporcional ao gradiente de factores angiogénicos. As fontes de factor pró-angiogénico são células em hipóxia. Este factor difunde-se através de um sistema tridimensional com a evolução temporal de T e é consumido por células endoteliais cuja proliferação é governada pelo parâmetro de ordem ϕ.

Vários parâmetros do modelo foram modificados de forma a verificar a sua influência na evolução do sistema. Tal como esperado, valores mais elevados de resposta quimiotáxica conduziram a um aumento do número de ramificações nos vasos, sendo eles mais finos. Valores mais elevados de taxa de proliferação conduziram a uma rede mais grossa e ramificada. Valores de células hipóxicas inicialmente adicionadas ao sistema maiores conduziram, tal como esperado, a maiores números de ramificações, maior consumo de factor angiogénico, vasos

mais longos e internamente mais proliferativos.

Alguns vídeos foram obtidos e encontram-se no CD em anexo que permite melhor ilustrar a evolução temporal do sistema nas diversas circunstâncias testadas.

Palavras-Chave: angiogénese, modelo de interface difusa, tridimensional, modelacao híbrida, VEGF

Abstract

Sprouting angiogenesis, the process by which new blood vessels grow from the pre-existing vasculature, is one of the central processes underlying vascular networks. It is implicated in more than 70 diseases so far, having become the object of study to many investigators, in the biological research field but also in the computational area. Since this is crucial for the development of cancers in its vascular phase, many researchers have dedicated the last 15 years to its study, which involves a great amount of different factors, in search of therapeutics eventually targeting angiogenesis.

Angiogenesis is a complex biological process. In this work we start by reviewing some of the main mechanisms essential to angiogenesis.

Various mathematical models to model angiogenesis combined with computational simulations have been proposed in the last 30 years, some in two-dimensional approaches, the most recent in 3D, and considering various different aspects involved in angiogenesis: chemotaxis, haptotaxis, angiopoietins and properties of the Extracelullar Matrix.

This thesis involves the simulation of a hybrid multi-scale phase-field model which describes the dynamics of the interface that divides the new capillaries and the stroma. Four equations model the behaviour of proliferating ECs in response to a gradient of a pro-angiogenic factor (T), leading to the growth and time evolution of a tree of vascular vessels from sprouts that emerge from the original capillar. These new sprouts are pulled by activated tip cells as a result of internal regulatory processes, and move with a velocity proportional to the gradient of angiogenic factors. The sources of pro-angiogenic factor are hypoxic cells. This factor diffuses throughout a three-dimensional system with the time evolution of T and is consumed by the ECs whose proliferation is governed by an order parameter ϕ.

Several parameters of the model were modified in order to verify their influence in the evolution of the system. As expected, higher values of chemotactic response led to an increase of the number of ramifications in the vessels, which were thinner. Higher values of proliferation rate led to thicker vessels and a more ramified network. Higher values of hypoxic cells initially added to the system conducted, as expected, to a higher number of branches, higher angiogenic factor

consumption, longer and internally more proliferative vessels.

Some videos were obtained and are in the CD attached which allow a better illustration of the time evolution of the system in the various studied circumstances.

Keywords: angiogenesis, phase-field model, three-dimensional, hybrid modelling, VEGF

Acknowledgements

I would like to thank Professor Rui Travasso for the support he provided me during this academic year, someone I already had the pleasure to be oriented by before, during a Computational Methods' subject of the Master Course in Biomedical Engineering. At the beginning of this year, his enthusiasm and passion by the computational investigation field were not new to me but soon became contagious and transformed this master project in a thrilling and exciting experience. I consider myself a richer person having had the opportunity to work with Professor Rui Travasso.

I must thank Professor Pedro Vieira Alberto for allowing me to actively participate in the classes of the Parallel Computation subject of the Master Degree in Modulation and Computational Simulation of Physics in the first semester of this year. I learned so much...

I also must thank Professor Fernando Nogueira for the several times he assisted me whenever a problem arose. Being part of the Center for Computational Physics was a constant support for me since 2009. During 2011, I participated in several meetings at IBILI, in the group coordinated by Doctor Paulo Pereira, which were very interesting and gave me an extra background of the biological processes concerning the wide topic of angiogenesis. I would like to thank this group for the opportunity.

The last year of the Master in Biomedical Engineering and these last months especially, are the culminating point of a stage of my life that I know I will not be able to live again. It is so the time to thank all the people that helped me throughout these years. A special thank to Professors Isabel Lopes and Miguel Morgado, for their support in and outside classes.

To my father José Luis, who sadly can not hug me with pride anymore, and my mother Olga Maria that has been everything, a special thank for allowing me to live the same magical effect the city of Coimbra brings into our lives, that they experienced thirty years ago. To my brother Luis Pedro I thank for the strength he represents. To Márcio, my boyfriend, best friend and best supporter, a great thank you.

I can not forget to express my gratitude to my friends Ana Cristina Leitão, Mariana Neto Costa, Ana Teresa Nunes, José Pinão, Tiago Cerqueira and Pedro Melo, without whom these five years would not have been the same. I thank you all for your friendship, advices and everything you taught me, in every way possible.

I thank the support of FCT through COMPETE for project PTDC/SAU-ENB/110354/2009.

Contents

List of Acronyms

EC Endothelial Cell

VEGF Vascular Endothelial Growth Factor

VEGFR1 Vascular Endothelial Growth Factor Receptor 1

VEGFR2 Vascular Endothelial Growth Factor Receptor 2

FGF Fibloblast Growth Factor

MMPs Matrix MetalloProteinases

EM Extracellular Matrix

PDGF Platelet-derived growth factor

SMC Smooth Muscle Cell

TGF Transformer Growth Factor

HIF-1 Hypoxic Inducible Factor-1

Ang-1 Angiopoietin-1

Ang-2 Angiopoietin-2

Dll1 Delta-like-1

Dll3 Delta-like-3

Dll4 Delta-like-4

Eph ephrin

NRP1 Neuropilin 1

NRP2 Neuropilin 2

List of Figures

List of Tables

Chapter 1

Introduction

1.1 Objectives and Personal Motivation

One of the main processes regulating the development of vascular networks and its morphology is sprouting angiogenesis, in which new blood vessels grow from the pre-existing vasculature [11].

Due to its implication in more than 70 disorders so far, in the past 15 years, there has been a growing interest in angiogenesis research among investigators from the biological field, leading scientists to the development of new therapeutic strategies, either to promote revascularization, to counterbalance or to reduce an angiogenic switch characteristic of some disorders [12]. In 1980 there were only 40 papers published concerning angiogenesis. In 2010, there were already nearly 6000 [5].

According to the Angiogenesis Foundation, the lives of at least 1 billion people worldwide could be improved with therapies targeting angiogenesis [5].

In some diseases, the excessive angiogenic stimulus which represents an uncontrolled process, leads to an enhanced neovascularization as in the case of inflammatory diseases such as rheumatoid arthritis, autoimmune diseases like psoriasis, during tumor development and in ocular disorders, as diabetic retinopathy [11]-[13]. These fragile new blood vessels lack vascular smooth muscle cells and are prone to rupture, remaining susceptible to hypoxic regulation and failing to become remodeled; these facts may lead to an inability to maintain a proper circulation [13]. In other disorders, however, there is an insufficient angiogenic stimulus which has numerous consequences namely the creation of dysfunctional ECs and vessels, and even the hindrance of vessel formation or healing. Ischaemic heart disease and preeclampsia are two examples [12].

The main goal of the work developed along the academic year that now reaches its end, was to computationally simulate the growth and time evolution of a vascular network in which new blood vessels grow directed by a tip cell according to the gradient of growth factors. This simulation was developed using Fortran 90 and was based on a phase-field model, fully described on chapter 3.

Finally, due to the colaboration between the Center for Computational Physics, through Professor Rui Travasso, and IBILI, the Institute of Biomedical Research in Light and Image, another goal of this project was conducted: the exchange of knowledge between the computational and the biological domains.

This thesis is integrated in the project "Angiogenesis in Diabetic Retinopathy: integrating experience and modelling" with reference PTDC/SAU-ENB/110354/2009, which is based in the interdisciplinarity between these two subjects.

There was also an initial objective of paralelizing the program or some of its subroutines with Message Passing Interface. Because of this initial goal, the Parallel Computation Classes of the Master Degree in Modulation and Computational Simulation of Physics were attended. However, because of the evolution of the project goals throughout the year which focused on the optimization of the program which lead to a relatively small amount of time needed for the simulation and also to the inclusion of other aspects of the process of angiogenesis in the simulation, this goal was excluded, being, however, a future objective.

In the next figure, the general schedule of the project is presented.

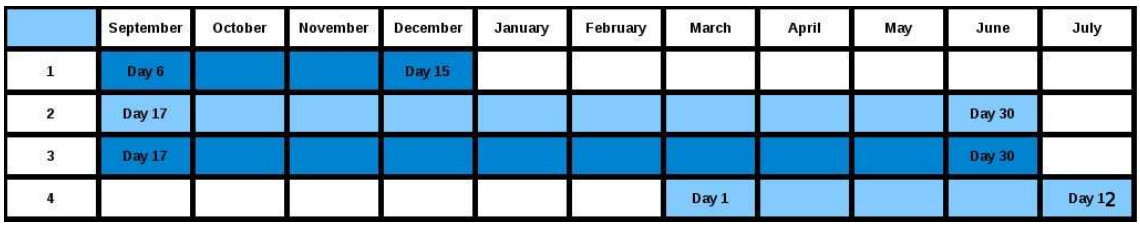

Figure 1.1: General schedule of the project.

1. Parallel Computation Classes
2. Program/Simulation Development
3. Bibliographic Research
4. Masther Thesis Elaboration

Chapter 2

Literature Review

2.1 General Aspects

Evolution has determined the existence of vascular systems with different complexities. In primitive species, such as the fruit fly *Drosophila melanogaster*, due to its size, anatomy and morphology of its respiratory system, oxygen diffuses throughout the small body, reaching all cells. In more complex species, which developed later and reach larger sizes, only the existence of a highly organized vascular network enables the distribution of oxygen and nutrients to all the cells, allowing the existence of these animals [12].

The discovery of the vascular system, in which the heart pumps the blood to all the parts of the body through arteries and to which the blood returns through veins after irrigating all the cells of every tissue, dates back to 1628, by William Harvey. Later, in 1661, Marcello Malphighi identified the capillaries as the smallest vessels existing between arteries and veins [12].

The entire vasculature surface is approximately 1000 m^2 and consists of large arteries which branch to originate pre-capillary arterioles that give rise to capillaries. The capillaries feed into venules which progressively associate into larger venous structures [13].

The Scottish anatomist and surgeon John Hunter was, in 1794, the first scientist to observe the proportionality between vascularity and metabolic requirements, in both health and disease, although the term angiogenesis only arose in 1935, when Herting described the formation of new blood vessels in the placenta. In 1971, Folkman studied the neovascularization inherent to the growth of solid tumors. The modern history of angiogenesis began [5, 13].

In humans, the first blood vessels appear in the embryo through a process called vasculogenesis, providing nutrition and trophic signals which promote organ morphogenesis. Not only the embryo, but also its extraembryonic membranes such as the yolk sac, develop during the early stages of life [14]. Capillaries are needed in all these tissues for exchange of nutrients and metabolites [5].

Vasculogenesis is the *de novo* blood vessel generation from vascular progenitor cells. It is the earliest morphogenetic process of vascular development and occurs exclusively during the early stages of the embryonic development, being associated with vascular endothelial progenitor cells [13]. During this process, endothelial progenitor cells organize themselves in blood clusters, which then fuse to form the primitive capillary plexus [13, 15].

A primitive vascular labyrinth of small capillaries is then extended as a result of the angiogenic process, which also involves sprouting, branching, splitting and differential growth of vessels; pericytes[1] and SMC cover the endothelial cell channels formed during vasculogenesis, resulting in a more complex, larger and more branched vascular network, that invades target tissues [12]-[15]. There are several intercellular signaling pathways involved in the processes of vasculogenesis and angiogenesis in mammals. Some of these pathways are the Vascular Endothelial Growth Factor pathway, the TGF-β pathway, the angiopoietin/Tie receptor pathway and the ephrin/Eph receptor pathway [14, 17, 18]. ECs are very versatile, having been observed to form tubular structures and ring type forms, by Folkman and Haundenschild in 1980, and these tubes were also seen to form a full network in 14 days [19].

As the embryo grows, some of the vessels originated in the primitive plexus remain as capillaries but others differentiate into arteries or veins, through a process which, interestingly, is thought to be intrinsically programmed, in which ECs, resulting from vasculogenesis, appear to have already at this stage acquired arterial and venous cell fates [12, 13].

Haemodynamic forces are believed to play a significant role in the processes of regression and differentiation of vascular vessels. These forces are generated by blood flow into a capillary segment. When the blood flow ceases and no more shear stress is exerted on the capillary walls of the vessel, there is a consequent regression of the vessel. When, instead, there is an increase in the shear stress and pressure in a vessel due to a greater amount of blood circulation inside it, a local recruitment of SMCs can lead to the differentiation of a capillary vessel into an artery or vein [13].

Shear stress or, in other words, haemodynamic forces originated by the blood flow in a vessel, occur as a molding force in the vasculature since whenever an arterial occlusion or a slowly progressing stenosis occur, a pressure gradient is generated along the shortest path in the interconnecting network leading to an increase in the blood flow velocity and consequently an increase in the fluid shear stress in these vessels which assume the function of "collaterals" [13]. There is a relationship between the diameter of an artery and the velocity of the blood flowing inside it, defined by the embryologist Thoma; any deviation from the relationship referred causes either vessel growth or its atrophy [13].

[1]Support cell for ECs that can differentiate into a fibroblast, a SMC or a macrophage [16].

During the process of sprouting angiogenesis, ECs from existing capillaries suffer a transition in their phenotype to tip cells. These cells detach from the vessels they were part of and migrate in the direction of the gradient of tissue produced growth factors. In this migration, another cell's phenotype, stalk cells, follow the tip cells [1, 11]. The existence of these two phenotypes of ECs is functionally fundamental since stalk cells guarantee the non-disintegration of the vessels and tip cells are essential to the formation of new vessels in the correct pattern [20].

During this process, vasodilatation, mediated by nitric oxide, occurs, simultaneously with an increasing of permeability allowing the extravasation of plasma proteins which have a relevant role in the migration of ECs [11]. Different architectures can occur: EC tubes commonly bifurcate and branch, but they can also fuse together through the *anastomoses*, establishing a micro-circulatory network [19].

In adults, angiogenesis occurs during the cycling ovary and pregnancy, in the placenta, and although ECs remain quiescent, they maintain the ability to divide rapidly if necessary, and, for example, in wound healing [1, 12, 13].

The process of angiogenesis may be summarized by the following five sequential steps [19]:

1. The capillary basal lamina dissolves through degradation by proteolytic enzymes produced by the filopodia of ECs;

2. ECs migrate and proliferate into connective tissues and the stroma in order to form sprouts;

3. Sprouts progress and originate the new blood vessels;

4. The basement membrane is resynthesized and the vessels' lumen is created;

5. A capillary network is originated by the occurence of anastomoses.

Arteriogenesis is the process following angiogenesis and describes the remodelling of the pre-existing anastomoses between arteries and arteriolas [21, 22]. This remodeling process includes the rapid proliferation of pre-existing collateral arteries, which are composed by a tube of ECs, internally covered by an elastic lamina and externally enfolded by SMCs and that can dramatically increase the lumen diameter, in an actively proliferation and remodeling process, to allow a greater perfusion in order to irrigate ischemic regions. These arteries are essential if an occlusion occurs. In this case, a pressure gradient is generated along the vessels neighboring the occluded zone that increases the velocity of the blood flow, causing an increase in the shear stress in these vessels which will, in these conditions, play the role of the collateral vessels [13, 22]. This process is not

a passive dilatation but an active one [13].

The following image summarizes the three processes involved in the development of the vascular networks discussed.

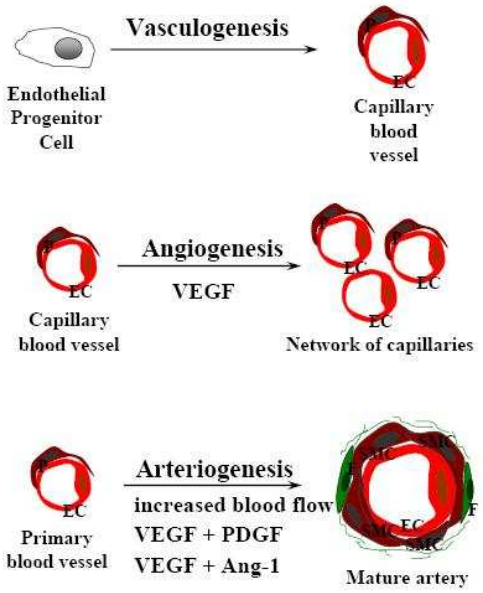

Figure 2.1: Vasculogenesis, Angiogenesis and Arteriogenesis. Vasculogenesis is characterized by an organization of angioblasts, the ECs precursor cells, angiogenesis is the process by which new blood vessels grow from the pre-existing vasculature and arteriogenesis is defined by a re-organization of the vascular network with the occurence of a hierarchy [4].

2.2 Biology Background

The proliferation and regression of the vasculature is highly influenced by oxygen, a central role molecule since it has an extreme importance in the feedback regulation of these processes [5].

Whenever oxygenation is not sufficient, hypoxic signals trigger or suppress various proangiogenic or antiangiogenic substances, leading to vascular growth. Cells begin to receive oxygen through the vasculature meanwhile generated, either by the increase of both the capillary surface area and maximum blood flow to the tissues, and also the reduction of the diffusion distances between capillaries and parenchymal cells. When the tissues receive the oxygen quantities needed, even during periods of peak metabolic activity, proangiogenic and antiangiogenic factors return to nearly normal levels, and these negative signals, in turn, stop the further development of the vasculature, closing the feedback loop. The opposite process is believed to take place when overoxygenation occurs [5].

The following figure shows the referred loop and in blue and red, the factors thought to be responsible for hypoxia (leading to vessel growth) and hyperoxia (leading to vessel regression), respectively [5].

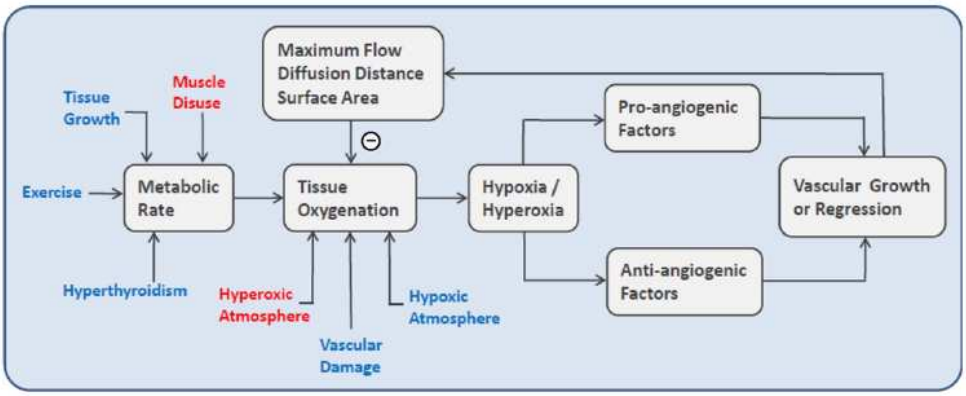

Figure 2.2: Oxygen role in vascular patterning. Hypoxia and hyperoxia states lead to vascular growth and regression, respectively, in a process in which the tissue oxygenation is subjected to a negative feedback loop [5].

In normal tissues and in pathological situations that lead to an angiogenic excessive stimulus, a break in the balance between angiogenic stimulators and anti-angiogenic factors occurs, which tips in favor of the pro-angiogenic factors.

VEGF is the best characterized pro-angiogenic factor which has a triple role in its vascular activity [1]:

1. Triggers the capillaries' permeability with the resulting activation of the tip cells' phenotype;

2. Foments the migration of tip cells according to its gradient;

3. Fuels the proliferation of stalk cells.

VEGF-A is produced by several types of parenchymal cells (myocytes, hepatocytes, neurons, astrocytes, etc.) in response to an hypoxic micro-environment [5].

There are various families of VEGF; VEGF-A was the first to be discovered.

VEGF-A was found, in 1992, by Shweiki *et al.*, to be strongly up-regulated in glial tumor cells exposed to an anoxic environment. This finding was also verified for *in vivo* and *in vitro* tests, and this state was reversed with cells' exposure to a non-hypoxic environment [5].
The VEGF ligands can join 3 primary receptors and 2 co-receptors. From the 3 primary receptors, only the VEGFR-1 and VEGFR-2 are associated with angiogenesis, VEGFR-3 is associated with lymphangiogenesis. The co-receptors, NRP-1 and NRP-2 are produced by ECs and are responsible for the increase in the affinity of the connections between the VEGF ligands and the primary receptors, although their influence on angiogenesis is still unknown [23].

There are 6 isoforms of human VEGF-1 (another designation for VEGF-A) known with 121, 145, 165, 183, 189 and 206 amino acids, being the VEGF165, VEGF121 and VEGF189 the most abundant and all sharing a common characteristic: the affinity to heparin, which is low in VEGF121, moderate in VEGF165 and high in VEGF189. The heparin binding property is important since it contributes to the anchorage of these VEGF isoforms to the extracellular matrix, hence contributing to a more active state of these isoforms [23].

VEGF is specific for ECs and is a potent chemoattractant and mitogen [9].

In figure 2.3, four rows are represented that express the various aspects characterizing the process of angiogenesis, where there is an imbalance in angiogenic factors favoring the pro-angiogenic factors side [6].

The first row compares the structure and functionality of normal and abnormal vasculature, for example a normal situation and a tumor vasculature. The second row of two-photon images shows that in the abnormal situation, a human carcinoma in mice, the vasculature is much more developed, showing that the pro-angiogenic stimulus created by the tumor hypoxic cells led to the increase in the vasculature in the vicinity of the tumor. Finally, the last two rows of figures show that there is an irregular deposition of pericytes in the abnormal vasculature when compared to the normal situation, which obviously, is due to the imbalance shown in the last row of figures [6].

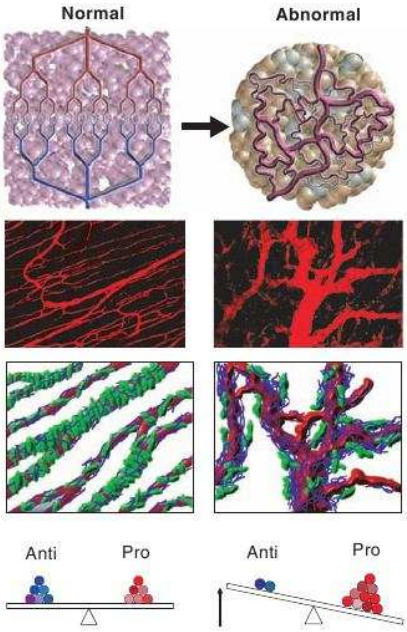

Figure 2.3: Normal and abnormal angiogenesis. Normal and abnormal angiogenesis differ on the organization of the vessels in arteries that ramify in arteriolas, which then ramify into capillaries, feeding into venules and, finally, veins; the blood flow is considerably increased in the abnormal situation in which there is also an irregular deposition of perycites due to the imbalance in the anti and proangiogenic stimuli [6].

VEGF is counterbalanced by angiogenic inhibitors as thrombospondin-1 [2] [6].

VEGF is detected by tip cells, the cells that pull new blood vessels, through their filopodia. Tip cell filopodia have three functions [24]:

- intercellular communication;
- cell migration;
- cell adhesion.

Filopodia exist in a various number of cells and play different roles, from the migration orientation in the growth cone of neurons to the signalling between cells in *Drosophila*. In endothelial cells, filopodia existing in tips are used to sense the VEGF gradient which tip cells follow and it is also probable that they use filopodia to attach to astrocytes or astrocyte-derived matrix (in retina) which produce a gradient of VEGF [24].

When there are enough filopodia on a tip cell anchored to the substratum, filopodia filaments of actin contract pulling the tip cell towards the VEGF stimulus. The proliferation of stalk cells and development of vacuoles within these

[2] Thrombospondin-1 inhibits angiogenesis through inhibition of Matrix MetalloProteinases

cells, lead to the elongation of the capillaries. When the tip cells of two or more capillary sprouts converge at the source of VEGF-A secretion (the hypoxic cell), the tip cells fuse together creating a continuous lumen which is able to allow the flow of oxygenated blood [5].

Gerhardt, *et al*, propose that tip cell filopodia extend on VEGF producing astrocytes and that VEGF-A stimulates tip cell filopodia, since the VEGF over-expression induces the extension of the filopodia, as well as vascular sprouting and also the hyperfusion of vessels in which the referred processes had already stopped. It is also, however, suggested by the authors that is is not clear whether if filopodial extension is regulated by VEGF or if it is an inherent characteristic of the tip cell phenotype, induced by VEGF [24].

Another important fact that relates VEGF and endothelial cell filopodia is that there is an increase of VEGFR2 on the filopodia of tip cells which is believed to be implicated in filopodia protrusion. It is concluded that the extension and maintenance of the filopodia existing in tip cells depends on VEGF-A signalling through VEGFR2 [24].

The important difference between the angiogenic stimulus in normal tissues and in pathological conditions is that in the second case the imbalance persists, there is a continuous production of VEGF and also of the proliferation of new blood vessels [1, 6].

The process of angiogenesis requires a very strict regulation of signals and, although VEGF is the pro-angiogenic factor to which more emphasis is given since it is included in the simulation, various other factors are essential to this process to occur correctly [1].

In some cancer types, for example, the central region of the spheroid mass becomes necrotic due to the the fact that the cells that constitute the interior part of the tumor are located too far from any blood vessels and the oxygen deliverage is less than the needed by these highly proliferative cells. In these cancer cells, apoptotic pathways are inactivated, anti-apoptotic pathways are activated, or invasion/metastasis pathways that promote escape from the hypoxic microenvironment are activated [25]. The cells that surround that area, still living cells, although hypoxic, may trigger a cascade of HIF-1 and VEGF mediated events that promote the vascularization of the tumor area through angiogenesis. HIF activation upregulates VEGF-A and its receptors VEGFR1 and VEGFR2 [20].

HIF is, so, another very important factor involved in angiogenesis [20].

Angiogenesis requires, as well, the degradation of the vascular basement membrane which occurs between the epithelial tissue and the connective tissue, so that ECs can migrate through the EM [19]. Tip migration is associated with the production of MMPs, a family of enzymes that proteolytically degrade

components of the EM, which, during angiogenesis, is remodeled in order to allow the migration of tip cells. Besides this, MMPs also have been shown to enhance angiogenesis, contributing to the pericyte detachment from vessels where angiogenesis is occuring and to the release of growth factors bounded to the EM. MMPs contribute to expose pro-angiogenic binding sites in the EM and cleaving the adhesions established between contiguous ECs. MMPs can also act to decrease angiogenesis through the generation of endogenous angiogenesis inhibitors [1, 6, 26]. Since the MMPs affect the affinity of VEGF species to different extracellular locations, this fact underlines the importance of this growth factor in angiogenesis [1].

Figure 2.4 shows the beginning of the process of sprouting angiogenesis: the ECs begin to loose the normally tight contacts with neighbouring cells and filopodia secrete large amounts of proteolytic enzymes; the basement membrane, the support layer that covers the endothelium, is degraded by these enzymes; tip cells migrate and penetrate the stroma; filopodia extend and follow the VEGF gradient during the migration of tip cells [7].

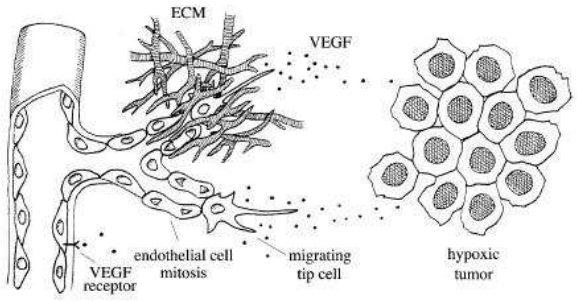

Figure 2.4: Early events of sprouting angiogenesis. The ECM is dissolved, new sprouts emerge from the original capillary pulled by tip cells in response to a gradient of VEGF produced by hypoxic tumor cells [7].

Tip cells activation is an essential process underlying angiogenesis, since they pull the new capillaries once activated.

Another important factor for the formation of new blood vessels and their stabilization is cell-adhesion. The adhesion junctions between contiguous cells are conducted by cadherins which inhibit the chemotaxis response of ECs to VEGF-A at the boundaries of two ECs, increasing the stability of those boundaries [20]. ECs, which like their precursors angioblasts are highly motile, have focal adhesion sites and can exert traction forces upon the matrix that surrounds them. Additionaly, they are polarized since they only move in the direction where filopodia exist. The cell adhesion hinders the motility of some ECs due to the bonds that exist between them and their neighbours [19].

Finally, two members of the angiopoietin family, Ang-1 and Ang-2, have shown to have a special role as regulators of angiogenesis. The angiopoietins are ligands

for the tyrosine-kinase receptor that exists in ECs, Tie-2 [9].

Figure 2.5 shows the Tie-2 signalling pathway.

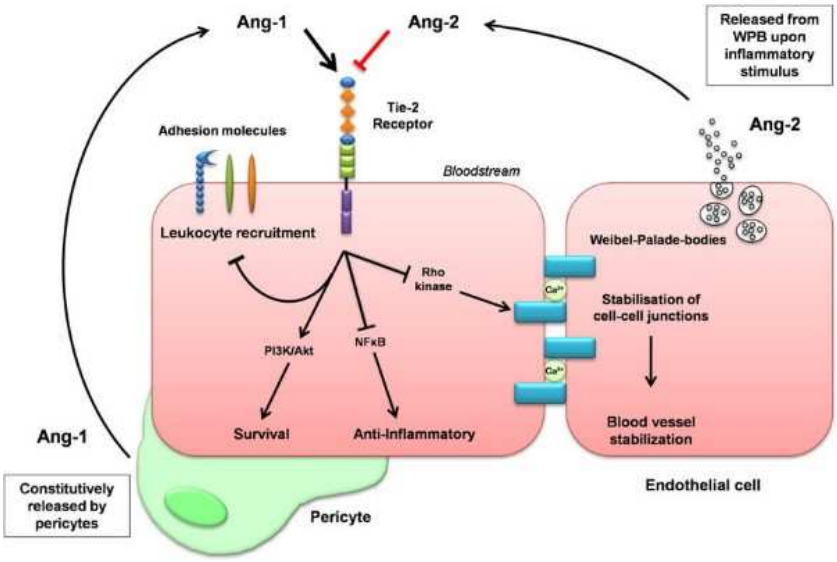

Figure 2.5: Tie-2 signalling pathway. Ang-1 and 2 bind to the tyrosine-kinase receptor Tie-2 with antagonistic effects, triggering important cell fate signalling pathways [8].

From this figure we can conclude that the tyrosine-kinase receptor Tie-2, to which both Ang-1 and Ang-2 bind, with an antagonist effect, triggers various cellular signalling pathways, such as PI3K/Akt which is extremelly important for the cell survival since it intervenes in several processes during the cell cycle as well as the NF-kB pathway, which is crucial during inflammatory processes [27].

Ang-1, which is secreted by peri-endothelial cells (pericytes and SMCs), has several functions related to angiogenesis [9]:

- maintains cell–cell interactions;
- inhibits apoptosis;
- is involved in the recruitment and sustainablity of support cells such as CMSs and pericytes, which are characteristic of the vessel maturation process;
- mediates interactions between the ECs and the basement membrane.

In embryos deprived of Ang-1 (or of the Tie-2 receptor), vasculogenesis occurs normally but angiogenesis is perturbed, although leading to the production of new vessels, they are leaky and inflamed [9].

Administration of Ang-1 causes a reduction on vessel permeability and an increase in vascular integrity [9].

Ang-2 is an antagonist of Ang-1 which binds the Tie-2 receptor, blocking the action of Ang-1. When subjected to the presence of Ang-2, cell-cell and cell-matrix connections are affected, and the basement membrane and the support cells loose the contact with the endothelium, leading to the occurence of malformations in the vessels. It is not widely expressed like Ang-1 since its expression is tighly regulated and is only observed in very strictly located regions where vascular remodelling is happening. Ang-2 is only expressed when ECs are activated, which can happen in response to a hypoxic stimulus, being released by the Weibel–Palade bodies, where it is stored [9, 28].

Ang-1 is, as referred widely expressed and not in response of a stimulus, and it is, so, responsible for the maintenance of the quiescent state of ECs. This state is modified with the local and temporal expression of Ang-2, which leads to a vascular remodelling. The regulatory effect of these angiopoietins is exerted over ECs in the presence or absence of VEGF. The co-expression of VEGF with Ang-2 (through binding to Tie-2 receptors) stimulates proliferation whereas in the absence of VEGF, ECs undergo apoptosis which results in the vessel regression [9].

The next figure schematically summarizes the discussed regulation performed by Ang-1 and Ang-2, and the effect of the presence and absence of VEGF simultaneously with the expression of Ang-2 [9].

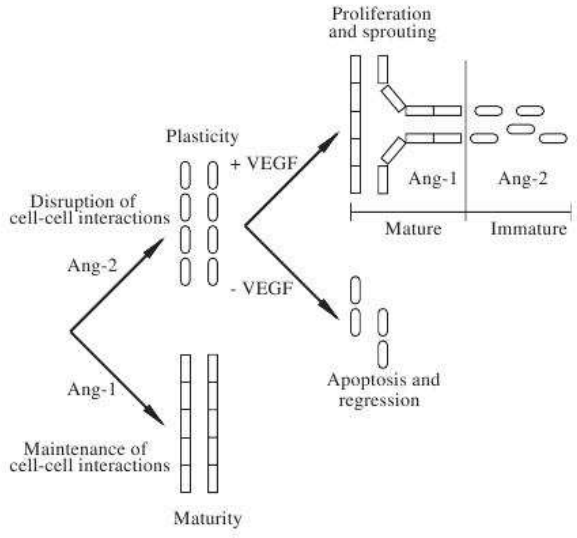

Figure 2.6: ECs regulation through Ang-1, Ang-2 and VEGF. Ang-1 is expressed and produced in a constant pattern by the tissue, whether Ang-2 is produced in certain circumstances, having a positive or negative effect depending on the VEGF concentration in the tissue [9].

2.3 The notch signaling pathway

Notch signaling is a relevant pathway to the regulation of cell fate decisions during the embryonic development of vertebrates and invertebrates, having been the subject in many studies suggesting to have important roles in various developmental processes [14, 22]. It was first studied in *Drosophila* [14].

Some of the processes in which this pathway is involved are apoptosis, differentiation, proliferation and oncogenesis [22].

Four notch genes have been described in mammals, Notch 1-4 and five ligands, Jagged 1 and 2 and DLL1, DLL3 and DLL4. Both receptors and ligands are expressed on the cell surface which contributes to notch signaling importance in the mediation of the comunications between adjacent cells [14, 22].

Notch is a large protein, having a single transmembrane domain which acts as a receptor for signalling using transmembrane proteins on the surface of adjacent cells. The stimulation of this pathway whose various sequential steps are illustrated in the following image, initiates a pathway which consists of transcriptional activation. Whenever a ligand binds the membrane receptor (the Delta in the next figure), notch is proteolytically cleaved and its intracellular domain is translocated into the nucleus. This domain will then interact with a transcriptional factor, the CSL in mammals, converting it to an activator of its target genes. The notch signalling pathway targets genes responsible for encoding other transcriptional regulatory proteins, determinant for cell fate [10].

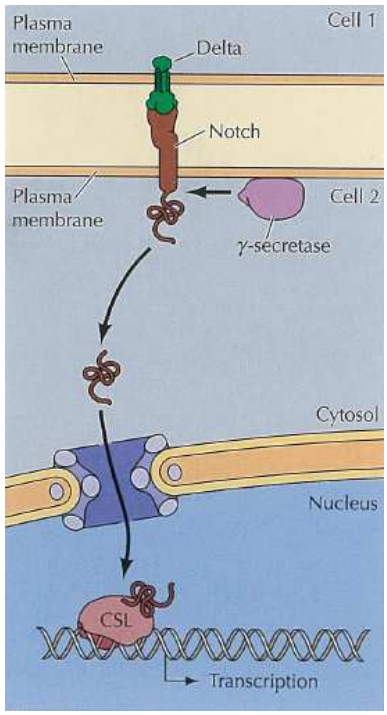

Figure 2.7: Notch Signalling Pathway. Adjacent cells interact through Delta ligands and the Notch receptor, leading to the nuclear transcription of important cell phenotype features [10]

In the case of notch signalling during angiogenesis, VEGF can induce the expression of the DLL4 ligand and the expression of Notch 1 and DLL4 through the PI3K-Akt pathway in ECs from human vessels. Therefore the activation of the pathway acts preventing an endothelial cell to adopt the tip cell phenotype if a tip cell is in its vicinity [1, 22].

Investigation carried out with respect to the embryonic expression of the Notch4 gene concluded that this gene's expression is restricted to vascular ECs and work developed concerning transgenic mouse models and tissue culture cells has proved that a mammary development is inhibited by the unregulated expression of the cytoplasmic domain of the Notch4 protein [14]. Studies suggest a partial functional redundancy of Notch1 and Notch4; although Notch4 gene is not essential, its mutation genetically interacts with a Notch1 mutation [22, 14].

Various mutations in the notch genes have been documented in the literature to be involved in pathologies related to vascular development. A mutation in the *Notch3* gene is associated to the human pathology CADASIL, an arteriopathy which causes stroke and vascular dementia. Also, mice lacking Jagged-1 or DLL1 were found to be embryonic lethal, showing severe vascular abnormalities. Furthermore, notch signaling modulates other pathways, namely, the PI3K-Akt and the NF-kB pathways [14, 22].

Notch has been associated with both oncogenic and tumor suppressive roles

and the existence of different phenotypes of mice used both in knockout and constitutive expression studies suggests the necessity of an extremelly tight regulation of this pathway [22].

2.4 Angiogenesis based Therapeutics

Researchers have undertaken intensive efforts to take advantage of the influence of angiogenesis in several disorders to develop clinical strategies concerning the pro-angiogenic potential of some growth factors like VEGF [12].

It is suggested that, although angiogenesis does not contribute to the initiation of a tumor, it is a factor that encourages its growth and, consequently, the inhibition of angiogenesis reduces the nutrient supply to a tumor, reducing its growth rate and the risk of metastasis [12, 29].

Due to this fact, scientists have dedicated their research to study various ways of inhibiting angiogenesis.

Due to the ECs stability, these cells were originally considered as the ideal target to antiangiogenic drugs, such as VEGF antagonists [12]. Also clinical trials are nowadays being carried out using inhibitors of MMPs that show an antiangiogenic action [26].

Avastin®(bevacizumab) is a Food and Drug Administration (FDA) approved therapy designed to inhibit angiogenesis developed by Genentech which provides an overall survival benefit in colorectal, breast and lung cancer patients when combined with conventional chemotherapy. This drug targets VEGF ligands, thus contributing to the inhibition of angiogenesis [22, 30].

However, anti-VEGF monotherapy was proved to be ineffective in humans, although it was effective in rodents; a fact that is still not understood [30].

Although showing promising results in some circumstances, anti-VEGF therapeutics have shown to induce tumor drug resistance after treatment, a process followed by the promotion of other pro-angiogenic mechanisms, which lead to the tumor's development [22].

The notch signaling pathway described in the previous section is another strategy under investigation by specialists since recent findings indicate a crucial role of this pathway in tumor angiogenesis, and could represent a novel approach to the anti-angiogenic therapeutics [22].

2.5 Mathematical Models Overview

In what concerns the computational field, several models concerning the process of angiogenesis have been presented in the literature, since, in the last 20 years, this topic has gained interest among the scientific comunity. This growing interest is strongly motivated by an increase in availability of biological data and improvement in computational facilities [29, 31].

Models of angiogenesis can be normally classified in the three following types: continuum, discrete and hybrid models [29, 31].

The continuum models are used to describe large-scale cell populations through systems of partial differential equations and, according to these models, capillary networks are described in terms of endothelial cell densities [29].

Although continuum models provide significant insight into the processes involving angiogenesis, they are significantly limited in what concerns the prediction of the formation of vascular structures. Vascular networks are described and presented as tree-like structures where sprouts appear to originate new blood vessels and, consequently, the models should recognize the existence of separate sprouts. This distinction is not established by continuum models and, so, a new model kind arises, the discrete model [29, 31].

Stokes and Lauffenburger were pioneers in describing angiogenesis using a discrete mathematical model. In their two-dimensional model, sprouts are defined by the trace of individual tip cells and branching by probabilistic rules. The migration of tip cells is defined by a stochastic differential equation which takes into account chemotaxis and random motion [32]. Several models were then presented in the literature using probabilistic rules to predict the displacement of tip cells, some in 2D and others, the extensions of those to 3D models [29, 31].

Although more useful when describing vascular structures such as sprouts, discrete models in which a network of individual space units is defined, represent an increase in the complexity of a model and time consumption of a simulation since every individual unit has its own parameters and processes such as proliferation or diffusion of factors.

Because of the convenience of both kinds of model in the various aspects that a mathematical modulation requires, hybrid models, combinations of continuum and discrete models, arose. The mathematical model described in the next chapter, in which the simulations presented are based, is a hybrid model as it combines a continuum approximation of angiogenic factors dynamics and endothelial stalk cell density through proliferation and a discrete representation of tip cells [29, 31].

The following paragraphs will focus on an analysis of the *state of the art* in what concerns mathematical models of angiogenesis, some of their differences,

comparisons between them and between the model presented.

Milde F, *et al*, present a 3D hybrid computational model of sprouting angiogenesis that considers both the effects of the EM and of the soluble and matrix-bound growth factors on the development of the growing capillaries. The authors discuss, mainly, the association between angiogenesis and tumor growth and proliferation, and also metastasis ocurrence in consequence of the detachment of tumor cell clusters' and migration through the existing vasculature to distant organs. Molecular species are represented by their concentration, migration endothelial tip cells by particles and new capillaries are represented by the endothelial cell density. In a very similar way, when compared to our model, the migration of ECs through the EM follows the chemotactic stimulus and defines the morphology of the newly formed sprouts. A trail of ECs is left on the 3D system. There are some important differences between both models since Milde, *et al*, consider a deposition of ECs in the EM which leads to the reduction of the diameter of the vessels as they approach their ends and considers other factors besides VEGF such as fibronectin (haptotactic response) and MMPs [29].

Holmes MJ and Sleeman BD present a mathematical model in which the viscoelastic nature of the EM is considered, unlike the models defined by Chaplain *et al.* (1995) and Chaplain and Stuart (1991,1993), that simulated the process of angiogenesis as the diffusion of ECs within a defined region of a passive EM. This interaction between the EM and the ECs is a very important feature of the process since it is a mechanism for maintaining endothelial new blood vessels and also to create the heterogeneous architectures that characterize the vascular networks [33, 34]. The simulation developed by Holmes MJ and Sleeman BD was a 2D simulation which considered the equations that describe continuous quantities, like the endothelial cell density, the EM density, the concentration of chemo-attractant and the concentration of haptotactic chemical, such as fibronectin, which is an adhesion mediator that enhances traction capabilities of ECs, via a system of partial differential equations [9, 19]. One disadvantage of this modelling approach is its inability to capture microscopic features of the process such as vessel branching and looping and the morphological properties of the emerging capillary network, features associated with discrete models [9].

Plank MJ *et al.* present a continuous 2D mathematical model of tumor angiogenesis that considers VEGF and the angiopoietins which have already been exposed in this work as important factors in the regulation of angiogenesis. In this article, the authors take into account the evolution of some quantities in response to the presence of a tumor. The EC density, concentration of VEGF and the concentrations of the angiopoietins 1 and 2 are taken into account in the model. The model considers that VEGF is produced at a constant rate by the hypoxic cells of the tumor and that it diffuses through the tissue, establishing a gradient. The ECs are divided into mature(inactivated) and immature(activated) cells. Although this assumption represents a simplification of the reality since cells' maturity should increase progressively, originating various intermediate maturation states,

the fundamental behaviour is taken into account and can be mathematically described. Immature cells produce Ang-2, the angiopoietin which is associated with located areas of high vascullar remodelling. Although the precise stimulus for Ang-2 expression is unclear, there is increasing evidence that suggests that Ang-2 is expressed especially at the tips of growing capillaries. The authors also consider that EC proliferation is confined to immature cells. For the maturation to take place it is considered that VEGF levels must be above a threshold. In what concerns Ang-1, the model establishes that it is present throughout the tissue at a constant level and that it is produced in a proportional fashion along with the density of mature EC. The action of both the angiopoietins is consistent with what is already known of their behaviour, and that is summarized in figure 2.6 [9].

Chapter 3

Description of the Model

3.1 General Aspects

This chapter briefly describes the hybrid model this simulation is based on, created by Travasso *et al.* [1]. Some of the aspects of this model were not considered in the simulation performed in 3D.

It is a multi-scale phase-field model which describes the dynamics of the interface that divides the new capillaries and the stroma.

Being a hybrid model of angiogenesis, continuous and discrete methodologies are underlying its mathematical equations. A discrete approach is concerned in the model during the description of the phenomena occuring at the cell level, such as tip cell activation and sprouting of new vessels. The continuum features of the model consist of the endothelial cell proliferation modelling and the tissue properties considered [1].

The biological background underlying the model is the same as that on the basis of this simulation. Blood vessels consist of ECs that have the hability to proliferate and, during an hypoxic stimulus, change their phenotype to tip cells in response to the action of internal mechanisms triggered by the referred environment. These cells lead to the growth of newly formed sprouts from original capillaries, being followed by stalk cells, the other ECs' phenotype that does not interfere with the direction and velocity of the new vessels, but necessarily proliferate in order to originate the vessel lumen which is essential for blood circulation to occur. This velocity is proportional to the existence of relevant growth factors like VEGF which, as a pro-angiogenic factor, leads the evolution of the process to an increase in the growth of ramifications and the formation of tree-like structures of capillaries. The action of this factor is counterbalanced by the action of other factors which instead act as angiogenesis inhibitors. During the process of angiogenesis, pro-angiogenic factors predominate [1].

Travasso *et al.* consider also the effect of the extracellular MMPs which, biologically, act remodeling the nearby EM, affecting the affinity of different

VEGF species relatively to the extracellular locations, consequently, affecting the bioavalilability of VEGF. VEGF exists in various isoforms which vary in the way they establish connections with the EM or with the cell surface, contributing to affect the vascular patterns [1]. The existence of different VEGF isoforms was not taken into account in this simulation neither the effect of the MMPs.

Travasso *et al.* considers the existence of other processes such as anastomoses [1].

Four equations model the behaviour of proliferating ECs in response to a gradient of a pro-angiogenic factor, leading to the growth and time evolution of a tree of vascular vessels from sprouts that emerge from the original capillar [1].

Travasso *et al.* model does not include the effect of haptotaxis, being the EM only the medium where ECs migrate with no adhesion sites. The activity of a balance between pro and anti-angiogenic factors is considered as well as the MMPs roles. It is a hybrid model which allows a faithful representation of the proliferation of ECs and the sprouts' formation, while being fast to integrate numerically, constituting an advantage over continuous models [1, 29]. The simulation carried out during this academic year introduces various inovative aspects. It represents the extension of the model created by Travasso *et al.* to a three-dimensional geometry and the program is completely optimized allowing the achievement of results in a relatively short period of time [1].

Finally, Travasso *et al.* develop a comparison between the model parameters and the experimentally measured quantities, an extremely important step in a simulation of this kind, but outside the scope of this project [1].

3.2 Mathematical Description

The mathematical model and computational simulation is based on four equations.

The first describes the dynamics of a factor T which consists of a balance between pro and anti-angiogenic factors that tips in favor of the pro-angiogenic factors, whenever angiogenesis occurs. The pro-angiogenic factor considered is VEGF. This growth factor is produced by tissue cells in hypoxia and released until oxygen reaches them through the blood flow inside nearby capillaries. Equation 3.1 describes the time evolution of the concentration of factor T as the combination of two terms.

$$\partial_t T = \nabla \cdot (D \, \nabla T) - \alpha_T \, T \, \phi \, \Theta(\phi), \tag{3.1}$$

where D is the diffusion constant of the factor T, α_T is the angiogenic factor consumption rate and $\Theta(\phi)$ is the Heaviside function. D might be considered as

a function if it depends on the type of angiogenic factors considered, since some of the isoforms attach to heparin, becoming the diffusion constant a function that depends on the position. This feature is not taken into account in this simulation but it is present in Travasso *et al.* modeling.

The Heaviside function takes value 1 when its argument, in this case, ϕ, is positive and 0 otherwise, guaranteeing the consumption to exist solely inside the capillaries. α_T is given by $\frac{D}{R_c^2}$, with R_c the radius of the ECs. The consumption rate of angiogenic factor depends on the diffusion constant of this factor and on the radius of the ECs since the capillary wall, composed by these cells, acts as a barrier to the angiogenic factor leading to the decay of its concentration on the order of the cell size. The obtention of the expression for α_T is achieved from the stationary solution of equation 3.2 close to the capillary boundary (see Appendix A).

This equation can be transformed into the simpler next expression, due to the fact that D is constant. The explanation and deduction are described in Appendix B.

$$\partial_t T = D\,\nabla^2 T - \alpha_T\, T\,\phi\,\Theta(\phi), \tag{3.2}$$

ϕ is the order parameter which distinguishes two distinct phases: the one that represents the interior of the capillary and the other that consists of the matrix outside the capillary. Initially, the capillary, with $\phi = 1$, corresponds to an aggregate of proliferative cells, the stalk cells, while at the outside of the capillary where $\phi = -1$, the cells are non-activated. The capillary wall separates these two phases thus having $\phi = 0$.

The time evolution of the order parameter ϕ is defined by the equation that follows from the deduction presented in Appendix C:

$$\partial_t \phi = M\,\nabla^2\left[-\phi + \phi^3 - \epsilon\,\nabla^2\phi\right] + \alpha_p\,(T)\,\phi\,\Theta(\phi), \tag{3.3}$$

where M is the ECs' mobility coefficient, ϵ is the width of the capillary wall and $\alpha_p(T)$ defines the proliferation rate of ECs. The right side of the equation is composed by two terms: the first is responsible for the maintenance of an interface that separates the two phases, the inside and the outside of the capillary. Because of the second term of this side of the equation, which describes the ECs' proliferation, the first term while allowing their proliferation, still assures the maintenance of a stable interface.

The proliferation rate $\alpha_p(T)$ depends on the value of T at every point of the system. For the points where $T < T_p$, this rate is given by $\alpha_p\, T$ and, when $T > T_p$ this rate reaches its highest value, $\alpha_p T_p$.

During the time evolution of the simulation, inside the capillary, ϕ maintains positive values, mainly because the capillary wall is defined by $\phi = 0$ and as an outcome of the interface dynamics term, which, as time evolves, contributes for the widening of the capillar. Only inside the capillary, equation 3.1 maintains the second term of the right side, as the Heaviside function becomes 0 when $\phi < 0$. Consequently, outside the capillary, equation 3.1 simply becomes:

$$\partial_t T = D\,\nabla^2 T, \tag{3.4}$$

which leads to the conclusion that, outside the capillar, the factor T diffuses over time through the system's geometry.

When $\phi > 0$, inside the capillary, the factor T also diffuses but is consumed at a rate α_T and with the consumption depending, also, on the concentration of T already existing and the concentration of the proliferative ECs, represented by ϕ.

A new sprout occurs from the original capillar, when some conditions are satisfied. These conditions will be fully clarified in the next section, where the computational approach to the model is presented and discussed. However, biologically, tip cells only acquire this phenotype whenever there are growth factors in their vicinity and they establish a gradient which allows the tip cell to move. Because of the notch pathway, only cells with no tip cells close to them can suffer this alteration of phenotype and become tip cells.

The activated tip cells, that will be the pulling force of new sprouts, move under the influence of a process called chemotaxis, with the velocity of their movement being proportional to the gradient of angiogenic factor, ∇T [1].

The next equation of the model describes the velocity of the tip cells:

$$\nu = \chi\,\nabla T, \tag{3.5}$$

where χ is the chemotactic response of the ECs. In Travasso *et al.*, this velocity was given by a more complex expression that considered the existence of a maximum value to the velocity. However, the results demonstrated a very small influence of the part of this equation that included the existence of a maximum value. Consequently, a simpler version of the velocity's expression was used in this simulation.

The last equation respects to the phase-field parameter ϕ of the tip cells. Since the value of this parameter is defined for the center of the tip cell, the parameter represents the evolution of the proliferation of the stalk cells in the neighborhood of the tip cells.

The tip cells are the ECs that have the ability to move during angiogenesis, producing an excess in cell density through their proliferation which is extended to the path they travel. This cell density obviously depends on the velocity of each

tip cell moving and evolves in an inversily proportional way with this velocity. The expression of the parameter ϕ developed by the tip cells is:

$$\phi_c = \frac{4\alpha_p(T)R_c}{3|\nu|}, \tag{3.6}$$

where $\alpha_p(T)$ defines the proliferation rate of endothelial cells, R_c is cell radius and $|\nu|$ is the absolute value of the velocity of the tip cells.

Appendix D presents the explanation that leads to the deduction of the previous equation.

3.3 Computational Approach

The 3D system considered in the simulation has a geometry of 60x100x100 and periodic boundary conditions.

An initial capillar was created defining the initial conditions to the order parameter ϕ. The values of ϕ were initially defined as 1 inside the capillar and -1 outside the capillar. The capillar radius was defined with the value of 5 and the vessel was aligned in the z direction, having a central axis characterized by $x = y = 50$.

In what concerns the initial conditions for the angiogenic factor T, 1000 angiogenic factor sources were initially randomly added to the system. Some of these were then withdrawn due to the fact that their position was in the oxygen diffusion area (they were positioned in the vascular network in a place at less than a distance of d from the original capillar) and they could not, consequently, represent hypoxic cells.

The values of ϕ and T were stored in two matrices with the same names. The coordinates of the hypoxic cells were registered in the *fontes* matrix.

Depending on the distance of these sources of angiogenic factor, hypoxic cells, to vessels, they will be kept and some will be withdrawn since the proximity to the oxygen existing inside nearby vessels reaches these cells satisfying their needs.

For all the positions of every point with $\phi > 0.9$ of the system (representing regions where blood is flowing), the distances to all the sources of angiogenic factor are calculated. In this step, one has to be careful with the implemented boundary conditions, which represent "mirror reflections" of the sources. If the smaller distance between the system point and the " reflections" of the hypoxic cell under analysis is less than the value of d, the production of this hypoxic cell is "turned off".

For every unit of the vascular network that is not a tip cell already chosen according to the conditions explained later in this report, an update in its values of T and ϕ is performed according to equations 3.2 and 3.3. In order to obtain the updated value of T in this point, the value of the diffusion constant D must be already defined. The laplacian of T is calculated using the discrete laplacian expression which consists in the quotient of the sum of the values of $T(x + \delta x)$ and $T(x - \delta x)$ minus twice the value of the value of $T(x)$ in the point itself, and the square of δx for all the three dimensions of the system: x, y and z. This expression was obtained using the Taylor series. Appendix E presents the deduction of this equation. The values of δx, δy and δz were defined as 1.

The final value of the updated T is obtained using the subtraction between the product of D by the laplacian of T, the product of the angiogenic consumption rate by the value of T, the value of ϕ and the Heaviside function which, as already referred, takes value of 1 when its argument is positive and 0 otherwise. Updated values of T of points outside the capillar, which have negative values of ϕ will consequently only suffer the influence of the first term of the right side of the equation.

The updated value of ϕ of this vascular network unit is obtained modelling equation 3.3 where the laplacian of ϕ, the laplacian of ϕ^3 and the laplacian of the laplacian (the biharmonic operator) of ϕ is also obtained following the same procedure as developed for the calculation of the updated value of T. The first term of the right side of the equation refers to the interface dynamics as discussed when the model was presented and the second term refers to the proliferation of stalk cells, which depends on the proliferation rate of these cells, the value of ϕ, this is, the amount of cells already existing in that point and the Heaviside function which guarantees that the second term of the right side of the equation is equal to 0 outside the capillar, where there are no ECs proliferating. The proliferation rate of the stalk cells depends on the value of angiogenic factor which has the fueling of the stalk cells proliferation as an important function [1].

For all the angiogenic sources that are located at a distance higher than d from a place where there is capillar, the value of T is set to 1 since they remain as hypoxic cells.

The time of execution of the program was defined to be limited at a value of 22.5 and the time step at 0.0005, resulting in the occurence of 45000 temporal iterations. Every 5 time iterations, the program selects new tip cells if some requirements are met.

The activated tip cells must obey the following conditions to be chosen to have that phenotype and for their activation to occur:

- The value of ϕ at the cell must be higher than 0.9;
- The value of T at the cell must be higher than T_c, the concentration of angiogenic factor that allows the branching;

- The absolute value of the vector gradient of T, $|\nabla T|$, calculated in the point, must be greater than G_m, the angiogenic factor gradient for branching;

- The cell is, finally, a tip cell if there is not any tip cell in a neighbourhood defined by a distance of 4 times the cells radius, R_c.

The center of the new cell must be located further than a cell radius length from the surface of the capillary.

T_c is a function of d, the oxygen diffusion area.

T_c is the upper limit for cell activation to occur. Extremelly high values of T_c lead to no tip cell activation, since the value of the T for branching to occur becomes unattainable. If, in the opposite situation, T_c is too low there will be a low value of T for activation of tip cells to occur, leading to a great amount of activated cells. The attainment of the expression for T_c is performed finding the steady state solution for T (continuous at a point a, which corresponds to the capillary wall), solving the equations in Appendix A.

Due to the fact that obtaining a computational solution of a stationary solution to the equation of T is a very slow process, in this simulation, an approximation was made for the value of T_c, which was defined as a constant value of 0.055, although the value produced by the resolution of the equations in Appendix A is different.

The first condition guarantees that the tip cell is chosen from the cells that are located inside the capillar, the second indicates the existence of angiogenic factor in the vicinity of the cell which is responsible for triggering EC's differentiation; the third condition assures the existence of a gradient of T which allows the tip cell to move and, the final condition, respects the notch signaling existing between cells and defines that a new tip cell only acquires that phenotype if there is not any tip cell immediately next to it, which represents a distance between the centers of the two cells of $4R_c$.

The first three conditions must be met at the center of the endothelial cell so that it can be classified with that phenotype, and because of the notch signalling pathway, the fourth and last condition must be obeyed since two neighboring cells can not be both tip cells.

The gradient of angiogenic factor is calculated through the calculation of the absolute value of the gradient vector. Each component of this vector in every dimension is reached by the subtraction of the value of $T(x + \delta x)$ and $T(x - \delta x)$, divided by twice the step, for the x case, according to the Taylor series. Appendix E presents the deduction of this equation.

Following the same procedure that characterizes the biological systems, whenever the chemotactic signal is low, the endothelial cell becomes a stalk cell again;

this is, when $T < Tc$ and $|\nabla T| < Gm$.

Every time the program ascertains the existence of cells fullfilling the four referred conditions, the points satisfying them are positioned in the matrix *tipcellslocal*. From all the cells which can constitute tip cells and that are in the *tipcellslocal* matrix, one is randomly chosen and added to the matrix *tipcellsglobal* of the program, where all the tip cells are saved.

The already chosen tip cells saved in the *tipcellsglobal* matrix, are moved in every time unit. The new positions are determined by the cells' velocity ν, which changes between two contiguous time units since the velocity is directly proportional to the gradient of T, which also changes in every time unit. The gradient of T is now calculated as the mean of the local gradients of T in the neighborhood defined by a sphere centered in the cell, with a radius equal to $2R_c$.

The velocity of the tip cells is proportional to the gradient of T, as already referred. The proportionality constant is χ, the chemotactic response of ECs which defines the magnitude of the ECs' movement triggered by the gradient of angiogenic factors. The new position is obtained by adding the product of the velocity and the time step to the previous position in all the three dimensions of the system. The velocity of the tip cells is kept in a matrix with the same name. Before the tip cells included in the *tipcellsglobal* are moved, the program ascertains whether the values of T and ∇T of that tip cells are higher than cut-off. If they are lower, the cell is no longer a tip, becomes a stalk cell and is removed from the *tipcellglobal matrix*. The matrix with the velocities of the tip cells is also updated.

The value of ϕ of the cells whose centers are located at a distance defined by R_c from the tip cells (the centers of the tip cells) already included in the *tipcellsglobal* matrix, are updated in every time unit using equation 3.6. In these circumstances, T evolves according to equation 3.4 as the model considers that at the tip cell, the angiogenic factors are not consumed, they only diffuse. For all the other points of the system, the update of the values of T and ϕ is performed through equations 3.2 and 3.3.

In every 5000 time unit intervals, the program produces three files that allow the attainment of a perspective of the time evolution of the important aspects considered in the simulation:

- The ECs' density that defines the tree-like vascular network with sprouts emerging from a central capillar;
- The active and angiogenic factor producing hypoxic cells and, finally,
- The space distribution of the angiogenic factor T.

The next table presents the list of parameters used in the simulation, a small

description and their values.

Table 3.1: List of Parameters and their Descriptions and Values in Simulation

Parameter	Description	Value in Simulation
ifinal	x dimension of the system	100
jfinal	y dimension of the system	100
kfinal	z dimension of the system	60
δ_x	x step size	1
δ_y	y step size	1
δ_z	z step size	1
R_c	Cells radius	4
χ	Chemotactic response of the ECs	1000
D	Diffusion constant	100
M	Endothelial cell mobility	1
α_T	Angiogenic factor consumption rate	6.25
α_P	Endothelial cell proliferation rate	1
ϵ	Interface width	1
T_p	Angiogenic factor concentration for highest proliferation	0.3
T_c	Angiogenic factor concentration for branching	0.055
capillar radius	Initial Radius of the capillar	5
d	Oxygen diffusion length	10
G_m	Angiogenic factor gradient for branching	0.01

Some of the parameters in the previous table are changed during the simulation in order to compare their effects on the obtained results.

The following code's flowchart schematically sumarizes the structure of the computational program and its behaviour.

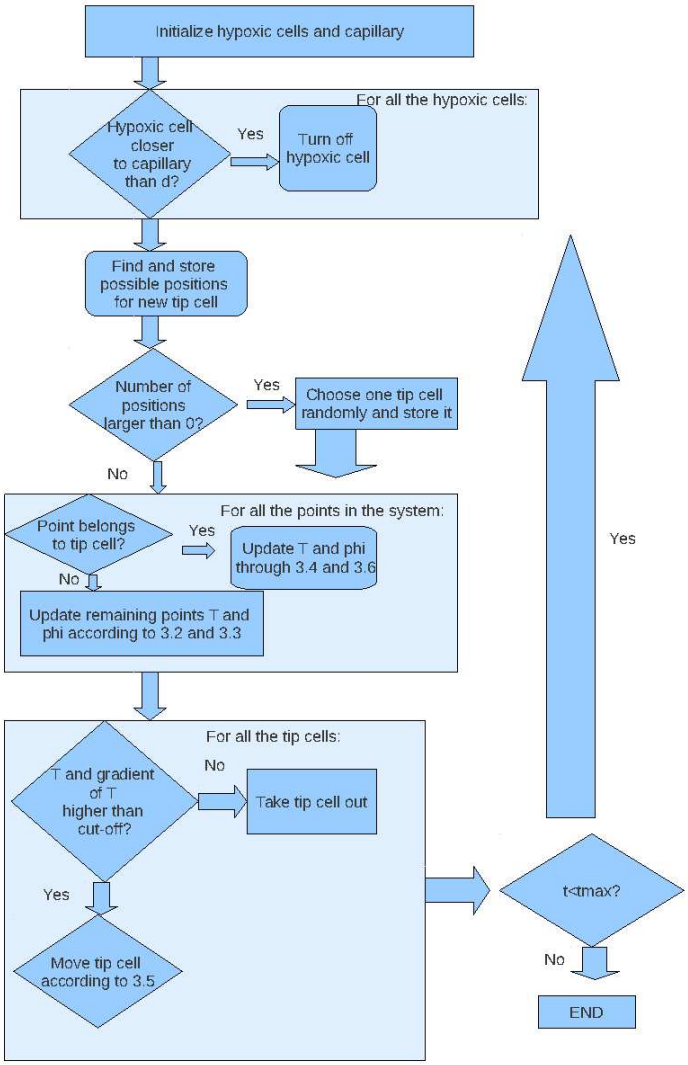

Figure 3.1: Code's Flowchart.

Chapter 4

Simulation's Results and Discussion

4.1 Initial conditions

The program was executed from $t = 0.0005$, the time step chosen that satisfies the equations of the model requirements for a viable simulation, to $t = 22.5$, which corresponds to 45000 temporal iterations.

In the following figures, comparisons between the effects of different parameters are presented. The discussion of these effects on the time and space evolutions of the system is also presented in this chapter.

In figure 4.1, the initial conditions for the parameter ϕ and the variable T are presented, for a number of sources of 500 and 1000.

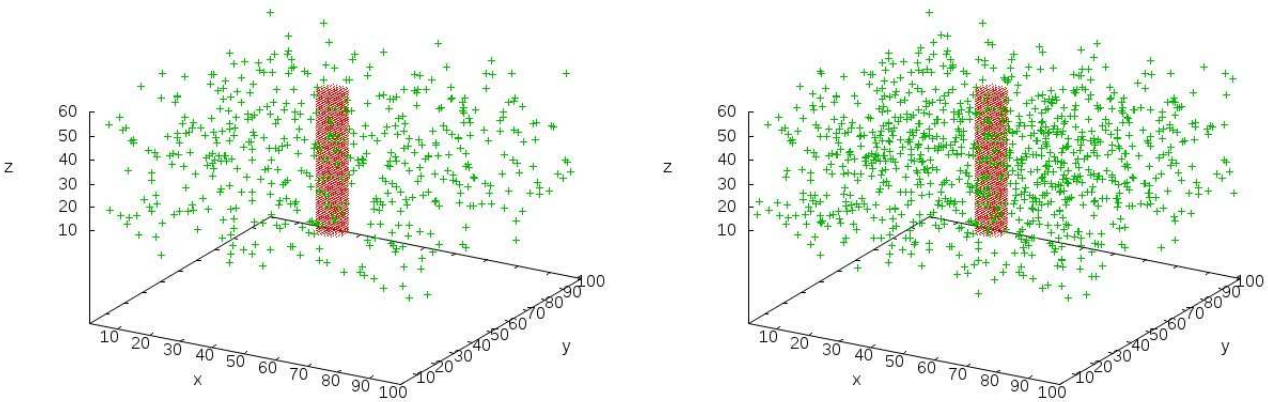

(a) (b)

Figure 4.1: (a) Initial conditions for ϕ and T, for $N = 500$ sources; (b) Initial conditions for ϕ and T, for $N = 1000$ sources.

The red dots represent values of $\phi = 1$, the initial capillar. The green crosses

are the 500 and 1000 angiogenic factor sources, hypoxic cells, at $t = 0$, respectively.

4.2 Analysis of the effect of the number of ang. factor sources on the system dynamics

Figure 4.2 shows the space distribution of the angiogenic factor sources 5000 and 45000 temporal iterations after the beginning of the simulation, for an initial value of sources equal to 500.

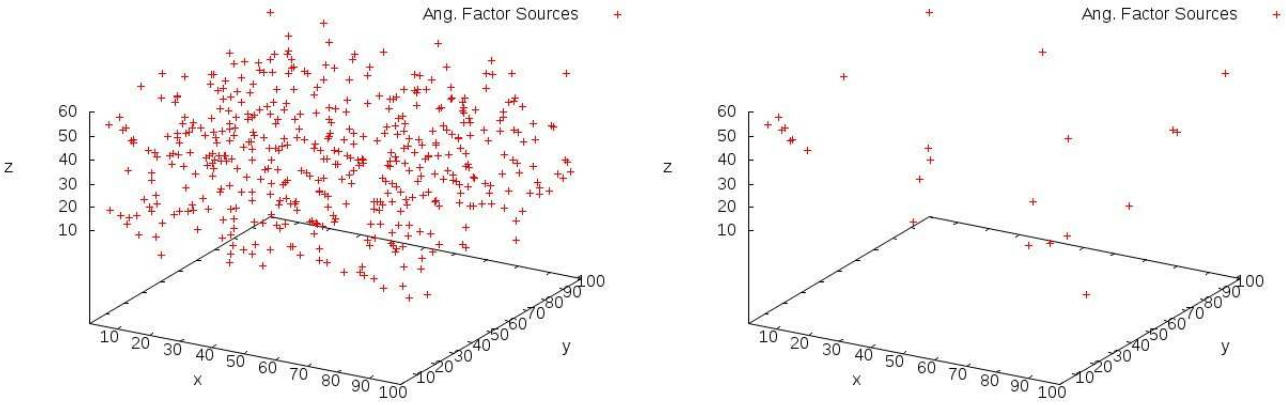

(a) (b)

Figure 4.2
(a) angiogenic factor sources for $t = 0.0005$ (5000 iterations), for $N = 500$; (b) angiogenic factor sources for $t = 22.5$ (45000 iterations), for $N = 500$.

At $t = 0.0005$, which corresponds to figure 4.2(a), some of the 500 angiogenic factor sources have already been withdrawn due to the fact that that their initial positions are in the oxygen diffusion area which, in these results, corresponds to the area defined by the distance of $d = 20$, from the capillar. The same is valid for the case of the existence of 1000 sources, represented in the figure 4.3.

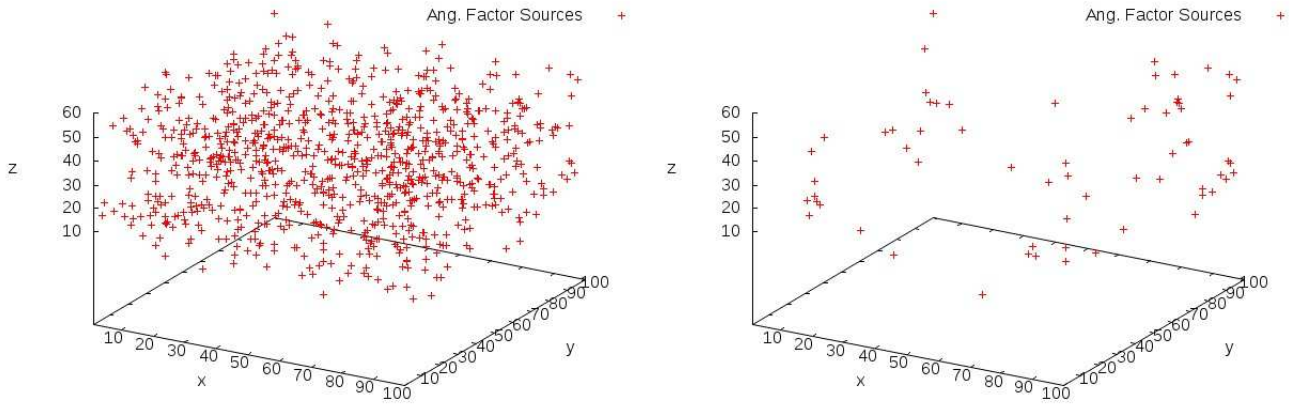

(a) (b)

Figure 4.3: (a) Angiogenic factor sources for $t = 0.0005$ (5000 iterations), for $N = 1000$; (b) Angiogenic factor sources for $t = 22.5$ (45000 iterations), for $N = 1000$.

With the model simulation, some of these points disappear since, with vessel sprouting resulting from the production and diffusion of T, the angiogenic factor balance, at each time iteration, some sources will be at a distance less than d from the nearby vessels, becoming, no longer, hypoxic cells.

45000 temporal iterations after, at $t = 22.5$, the distribution of angiogenic factor sources is represented in figures 4.2(b) and 4.3(b), for initial values of sources of 500 and 1000, respectively.

Figures 4.2 and 4.3 were obtained for the following parameters:

- $d = 20$
- $\alpha_P = 1.0$
- $\chi = 1000$

Every 5000 iterations, the program saves the positions of the hypoxic cells in a file. The 9 files obtained were combined in a video that illustrates the evolution of the sources with time. The files $N500.gif$ and $N1000.gif$ in the attached CD are the videos representing the time evolution of the hypoxic cells for initial numbers of 500 and 1000 hypoxic cells, respectively.

9 files with the time evolution of the parameter ϕ and of T are also obtained for each case. The next paragraphs will compare the influence of a difference in the initial numbers of hypoxic cells added to the system on its evolution.

The following figure shows the time evolution of the parameter ϕ for 5000, 25000, 35000 and 45000 iterations, for $N = 500$, $d = 20$, $\alpha_P = 1.0$ and $\chi = 1000$.

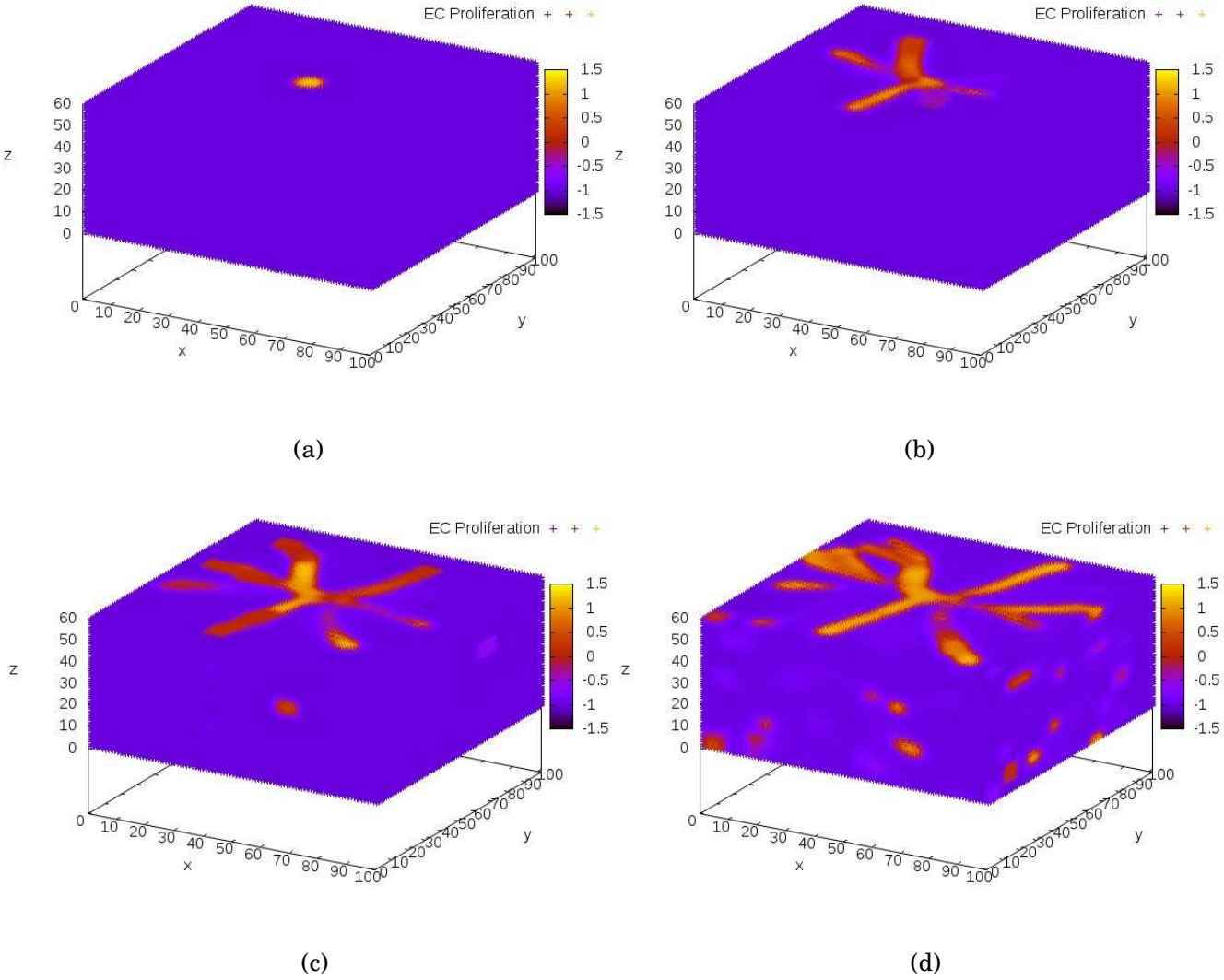

Figure 4.4: Parameter ϕ for (a) 5000; (b) 25000; (c) 35000; (d) 45000 iterations; for $N = 500$. Lower values of angiogenic factor sources lead to less sprouting and less proliferative vessels.

The following figure shows the time evolution of the parameter ϕ for 5000, 25000, 35000 and 45000 iterations, for $N = 1000$, $d = 20$, $\alpha_P = 1.0$ and $\chi = 1000$.

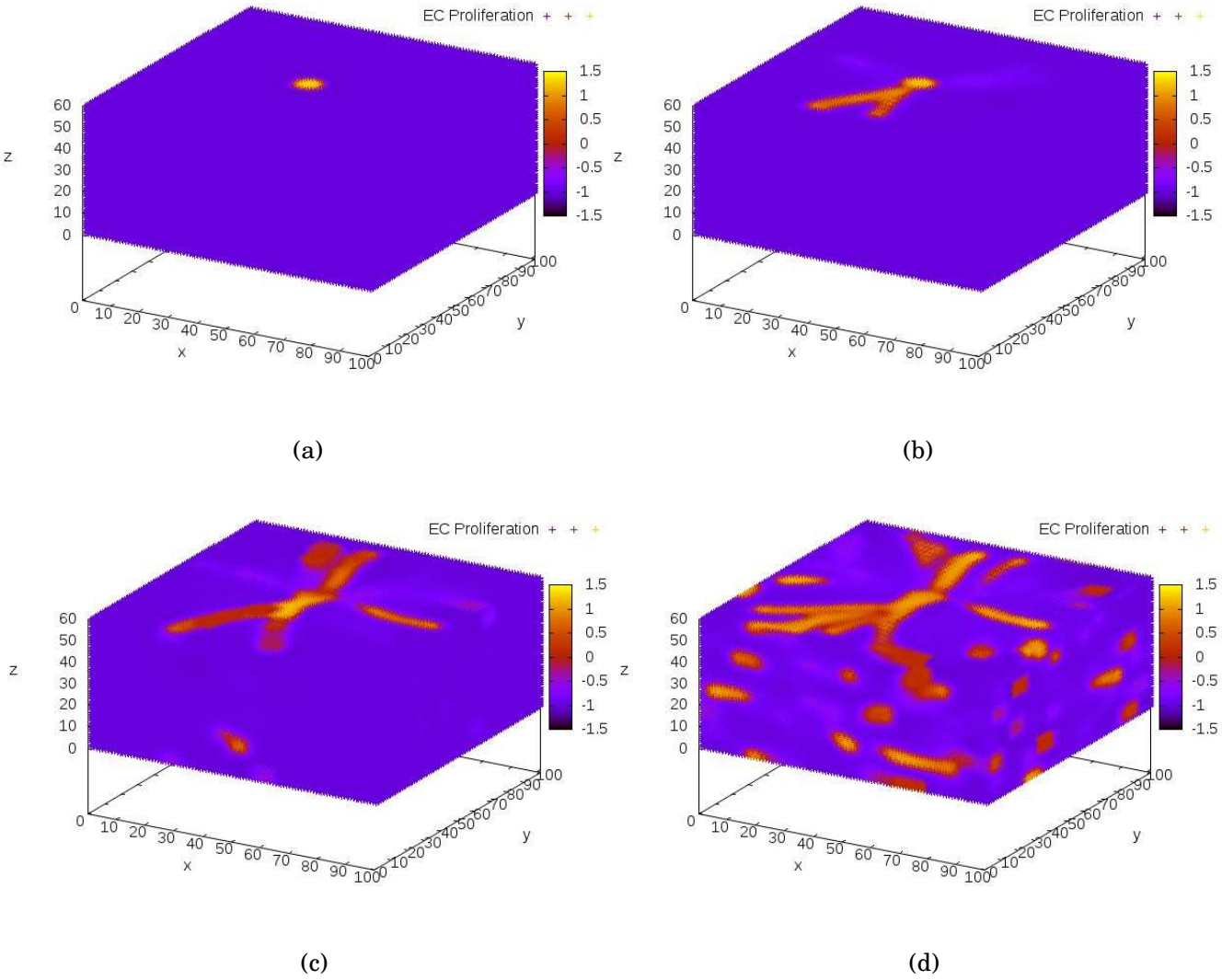

Figure 4.5: Parameter ϕ for (a) 5000; (b) 25000; (c) 35000; (d) 45000 iterations; for $N = 1000$. Higher values of angiogenic factor sources lead to higher sprouting and greater proliferative vessels.

From the previous images, we can observe that, a the number of hypoxic cells higher consequently leads to an increase in the production of angiogenic factor T. After 5000 iterations of the start of the simulation, there is no sprouting in both cases and, after 25000 iterations, although in both cases sprouting occurs, the interior part of the central vessel and its ramifications has already values between 1 and 1.5, for $N = 1000$, which is a sign of high proliferation of the vessels. The ECs' proliferation, combined with the existence of a gradient of angiogenic factor, leads to the occurence of sprouting of the vessels from the original capillar earlier and with a higher magnitude. Figures 4.4(c) and 4.5(c) already show a proliferative vessel in the case where $N = 500$, although, when compared to the case of figure

4.5(c), where $N = 1000$, more vessels are approaching the system's boundaries. Finally, in figures 4.4(d) and 4.5(d), it becomes clear that, for $N = 1000$, the vessels have higher values of ϕ due to a higher proliferation and they are more frequent.

The following figure shows the time evolution of the points with $\phi > 0$, points where there is capillar, for 5000, 25000, 35000 and 45000 iterations, for $N = 500$, $d = 20$, $\alpha_P = 1.0$ and $\chi = 1000$.

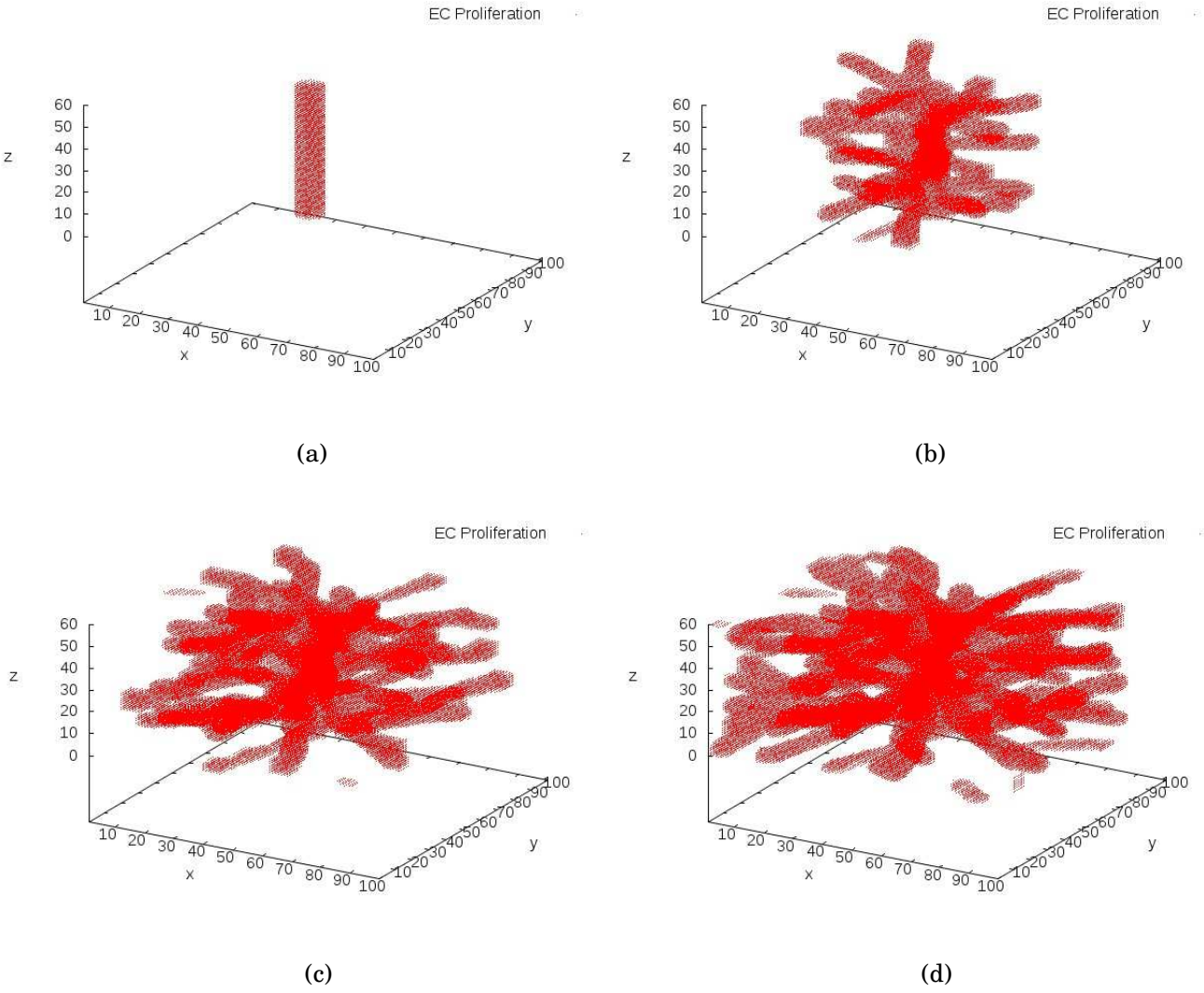

(a) (b)

(c) (d)

Figure 4.6: Time evolution of the points with $\phi > 0$, points where there is capillar for (a) 5000; (b) 25000; (c) 35000; (d) 45000 iterations, for $N = 500$. Lower values of angiogenic factor sources lead to less sprouting.

The following figure shows the time evolution of the points with $\phi > 0$, points where there is capillar, for 5000, 25000, 35000 and 45000 iterations, for $N = 1000$, $d = 20$, $\alpha_P = 1.0$ and $\chi = 1000$.

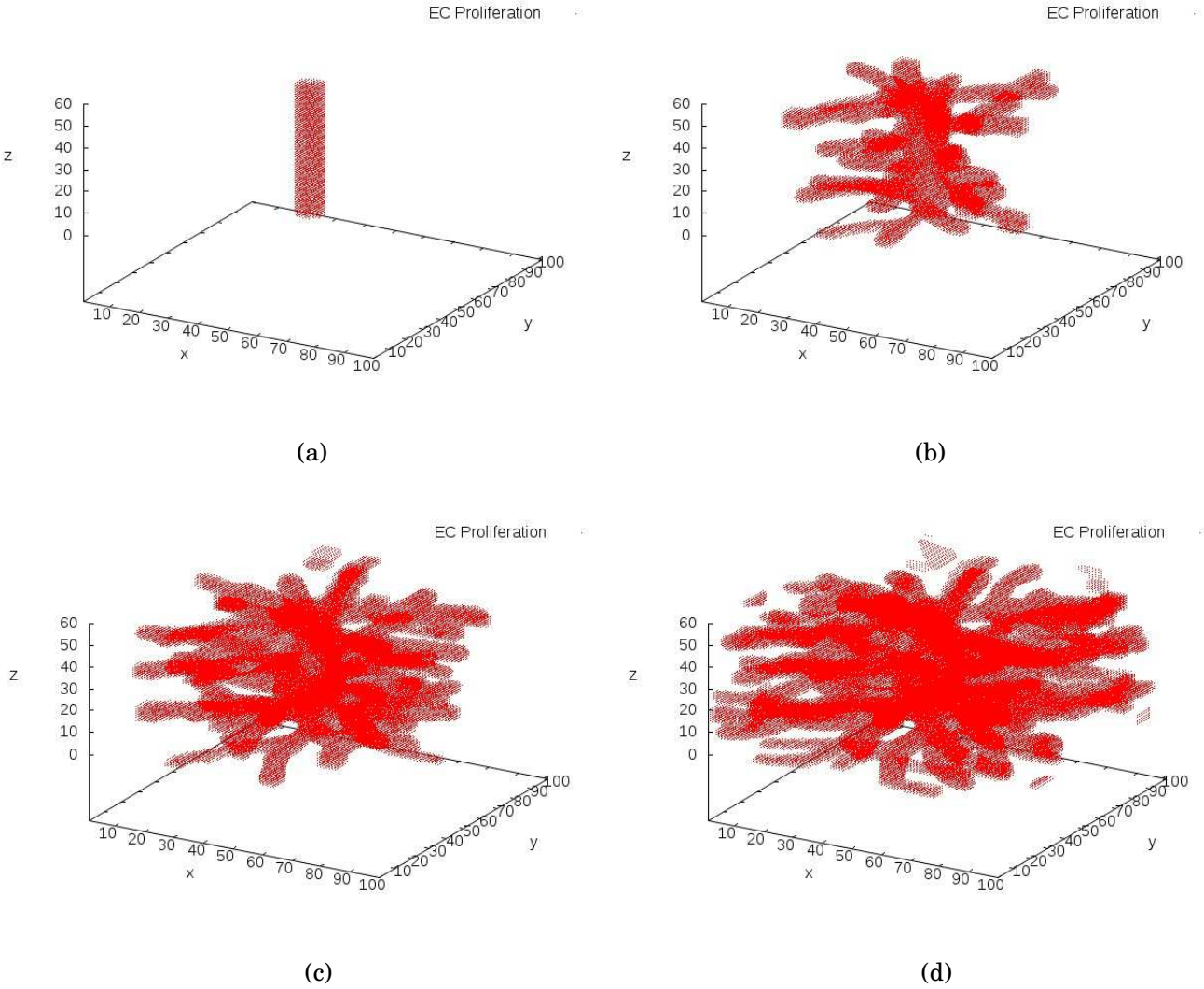

(a) (b)

(c) (d)

Figure 4.7: Time evolution of the points with $\phi > 0$, points where there is capillar for (a) 5000; (b) 25000; (c) 35000; (d) 45000 iterations, for $N = 1000$. Higher values of angiogenic factor sources lead to higher sprouting.

The previous images are also dedicated to the analysis of the parameter ϕ but only for the points with values higher than 0 are ilustrated. These points represent the tree of sprouts that emerge from the initial capillar. In these figures, the previous conclusions become clearer.

The following images also analyse the situation described but in what concerns the variable T.

The following figure shows the time evolution of the variable T for 5000, 25000, 35000 and 45000 iterations, for $N = 500$, $d = 20$, $\alpha_P = 1.0$ and $\chi = 1000$.

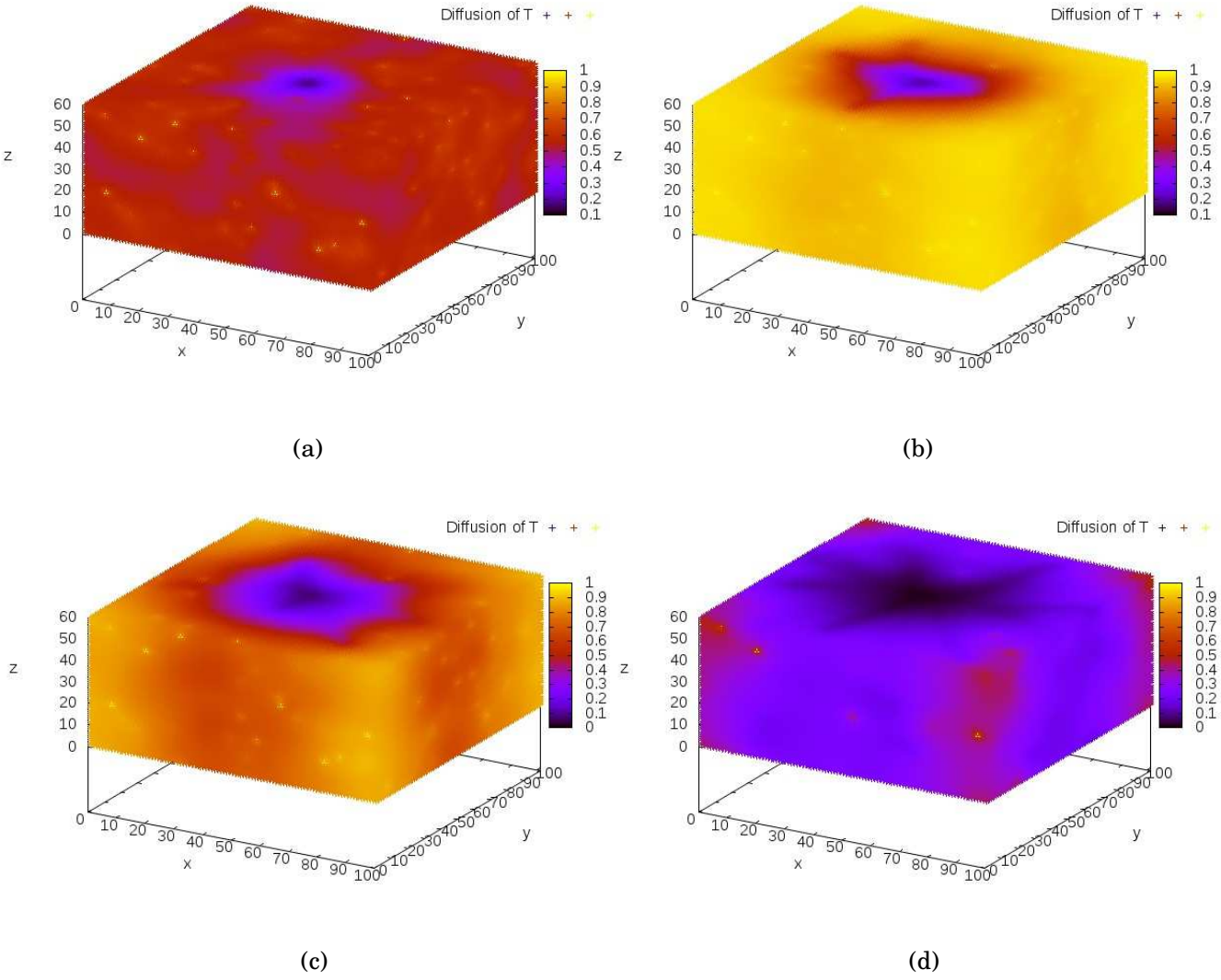

Figure 4.8: Parameter T for (a) 5000; (b) 25000; (c) 35000; (d) 45000 iterations; for $N = 500$. Lower values of angiogenic factor sources lead to lower angiogenic factor consumption.

The following figure shows the time evolution of the variable T for 5000, 25000, 35000 and 45000 iterations, for $N = 1000$, $d = 20$, $\alpha_P = 1.0$ and $\chi = 1000$.

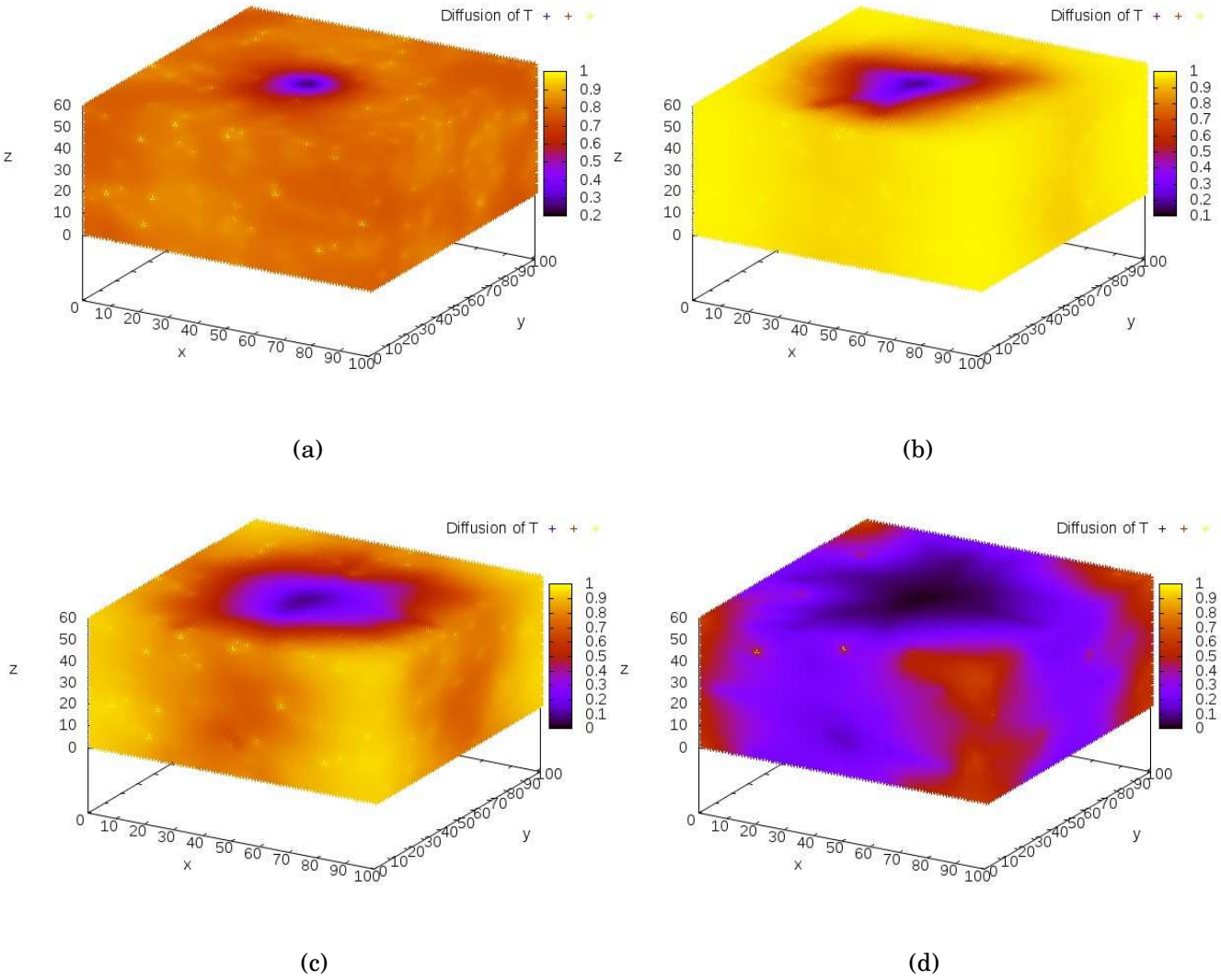

Figure 4.9: Parameter T for (a) 5000; (b) 25000; (c) 35000; (d) 45000 iterations, for $N = 1000$. Higher values of angiogenic factor sources lead to higher angiogenic factor consumption.

The previous images show that, as expected, for $N = 500$, at 5000 iterations, the values of T of the system are lower than those for $N = 1000$. The color scale shows the prevalence of the red color which represents values from 5.5 to 6.5, rather than the orange in the $N = 1000$ figure, where the values are between 0.7 and 0.9. In both figures, the yellow dots represent the angiogenic factor sources, hypoxic cells, which have values of T equal to 1. In both figures 4.8(a) and 4.9(a)

there is no spouting occuring yet since the lower values of T, which occur in the central region of the figure and represent the initial vessel, are confined to this area. The vessel has values between 0 and 0.4, the lowest in both graphs, since the angiogenic factor in this region, unlike in the rest of the 3D system, not only diffuses according to equation 3.2, but is also consumed.

20000 time iterations after, the occurence of sprouting in both graphs is clear due to the extension of the lower values to the ramifications already seen in the previous figures for the evolution of the ϕ parameter. Nevertheless, outside the capillar tree, we see that the values of T are higher for $N = 1000$ than for $N = 500$, as expected. The same pattern is observed for 35000 iterations.

Figures 4.8(d) and 4.9(d) already show a considerable part of the 3D system with low values of T due to the sprouting that extends these values from the center of the system to its boundaries being, again, the values of T for $N = 1000$ higher than those for N=500, although the spouting effect on T is not so clear than in figures 4.7 and 4.6.

The files $N500phi.gif$, $N500T.gif$, $N1000phi.gif$ and $N1000T.gif$ show the videos of the time evolution of the values of ϕ and T, for $N = 500$ and $N = 1000$, respectively, from 5000 to 45000 temporal iterations.

4.3 Analysis of the effect of the proliferation rate α_P on the system dynamics

Two values of α_P, the ECs' proliferation, are used in the simulations, 1.0 and 2.0.

We expect that, for $\alpha_P = 1.0$, since the EC's proliferation is lower, a lower number of ramifications and thiner vessels occur comparatively to $\alpha_P = 2.0$.

The parameters used in the following figures were:

- $d = 20$
- $N = 1000$
- $\chi = 1000$

The following images show the ϕ distributions in the 3D system for $\alpha_P = 1.0$ and $\alpha_P = 2.0$.

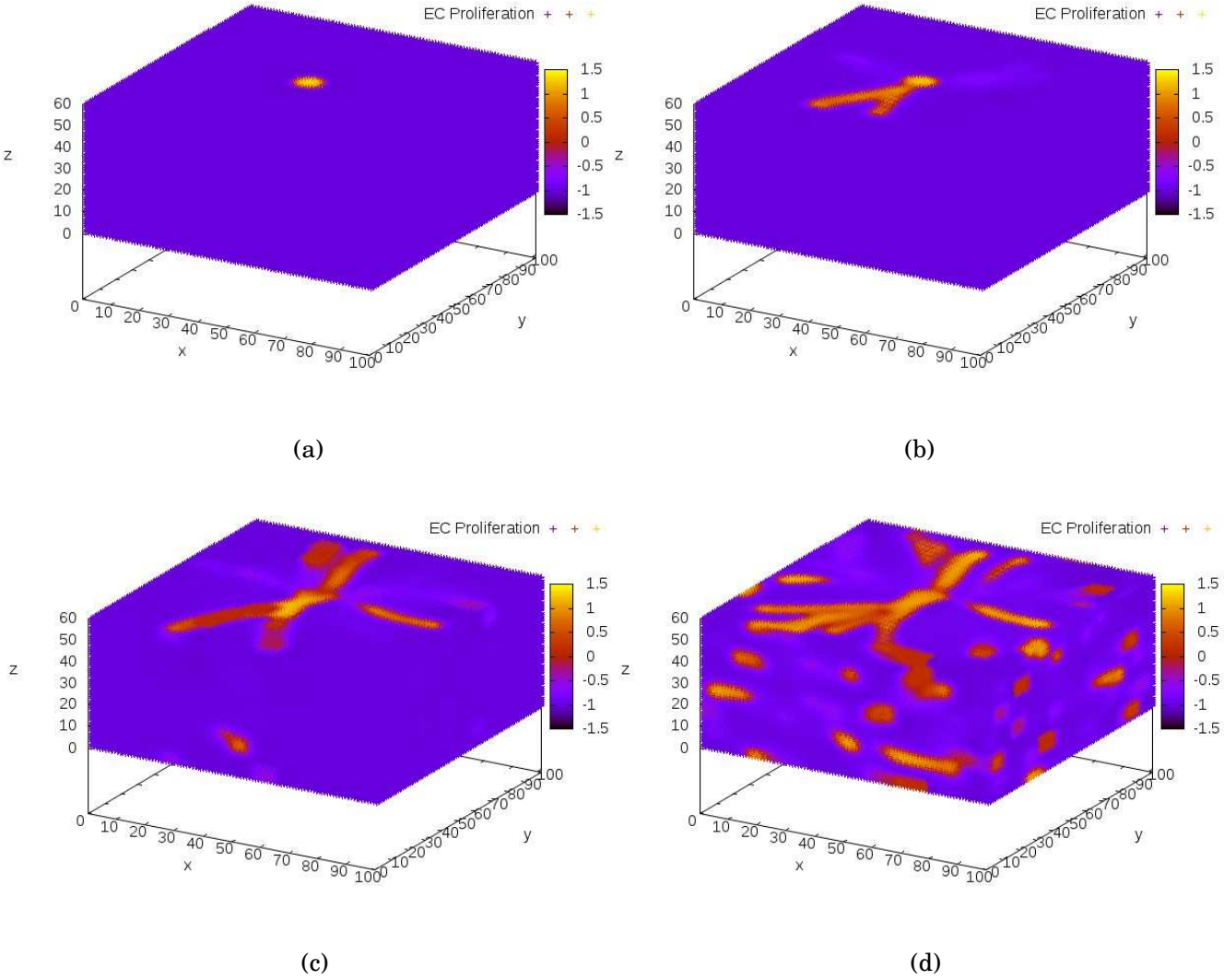

Figure 4.10: Parameter ϕ for (a) 5000; (b) 25000; (c) 35000; (d) 45000 iterations, for $\alpha_P = 1.0$. Lower values of proliferation rate lead to thinner, less proliferative and ramified vessels.

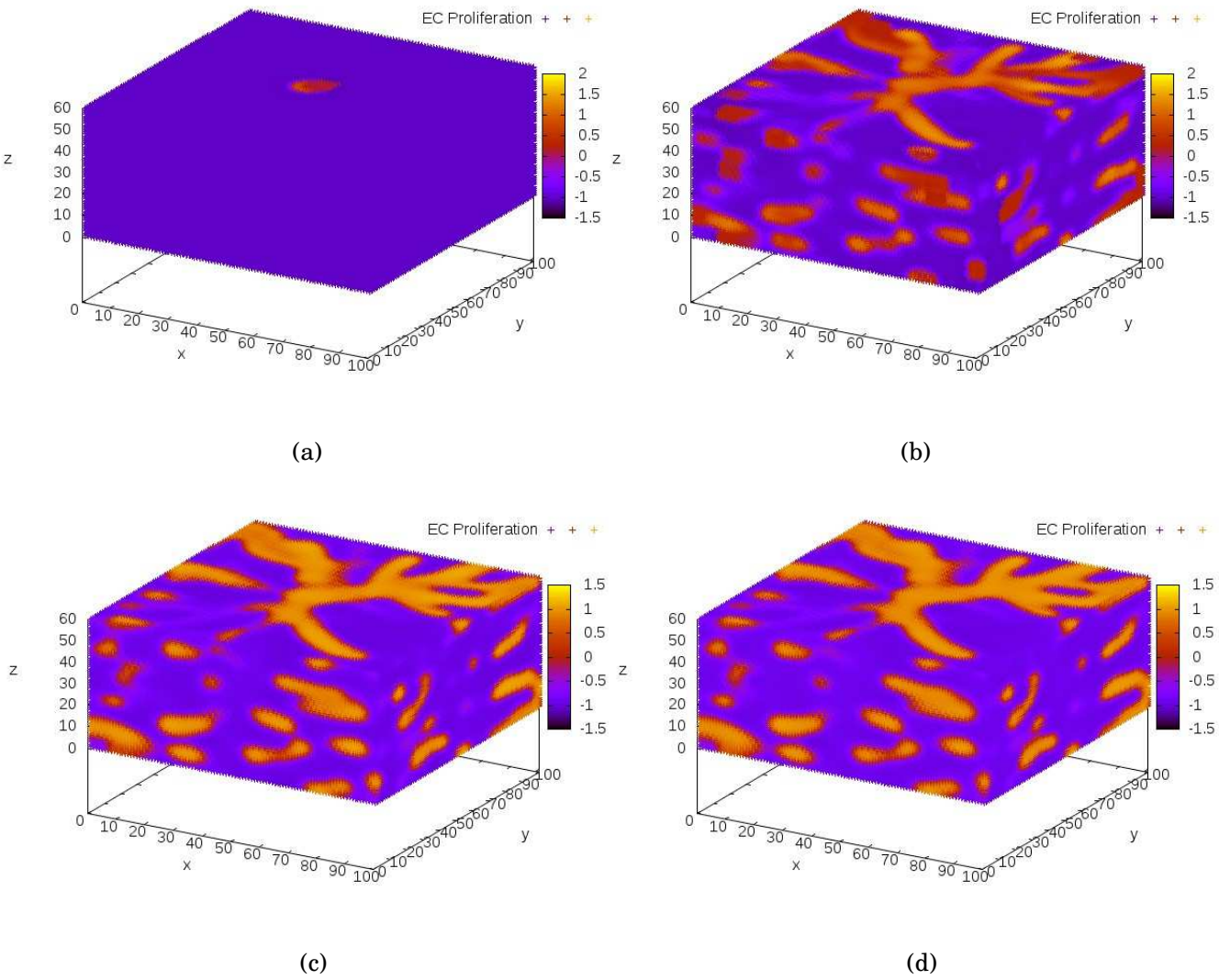

Figure 4.11: Parameter ϕ for (a) 5000; (b) 25000; (c) 35000; (d) 45000 iterations, for $\alpha_P = 2.0$. Higher values of proliferation rate lead to thicker, more proliferative and ramified vessels.

The files $alphaT1.0phi.gif$ and $alphaT2.0phi.gif$ in the attached CD are the videos of the time evolution of the values of ϕ for $\alpha_P = 1.0$ and $\alpha_P = 2.0$, respectively, from 5000 to 45000 temporal iterations.

Figures 4.10 and 4.11 show the referred expected aspects. A higher proliferation rate leads to higher values of ϕ which are represented by the prevalence of the yellow color inside the vessels when $\alpha_P = 2.0$, higher number of ramifications and thicker vessels.

In this analysis, the tree figures are not shown since the referred aspects are more evident in the previous figures.

In what concerns the evolution of T, it is expected that, since a higher proliferation leads to an increase in the number and thickness of the sprouts, the values of T will evolve resulting in lower values of this parameter since the angiogenic factor represented by the parameter T is more consumed by the generated vessels.

The following figures show the evolution of the parameter T for both the considered α_P values and for 5000, 25000, 35000 and 45000 temporal iterations.

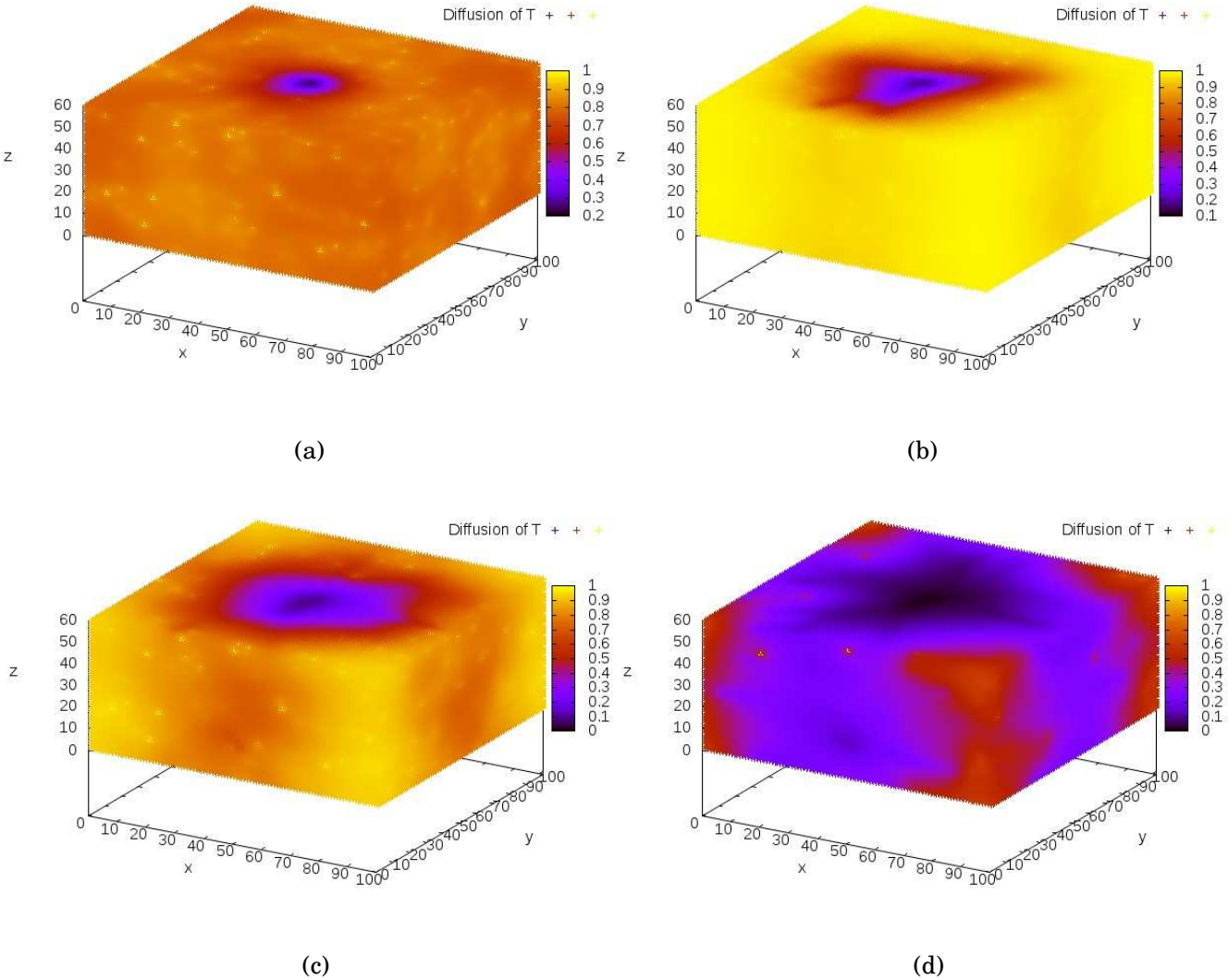

Figure 4.12: Parameter T for (a) 5000; (b) 25000; (c) 35000; (d) 45000 iterations, for $\alpha_P = 1.0$. Lower values of proliferation rate lead to a distribution of the parameter T with higher values comparing to a higher value of proliferation rate.

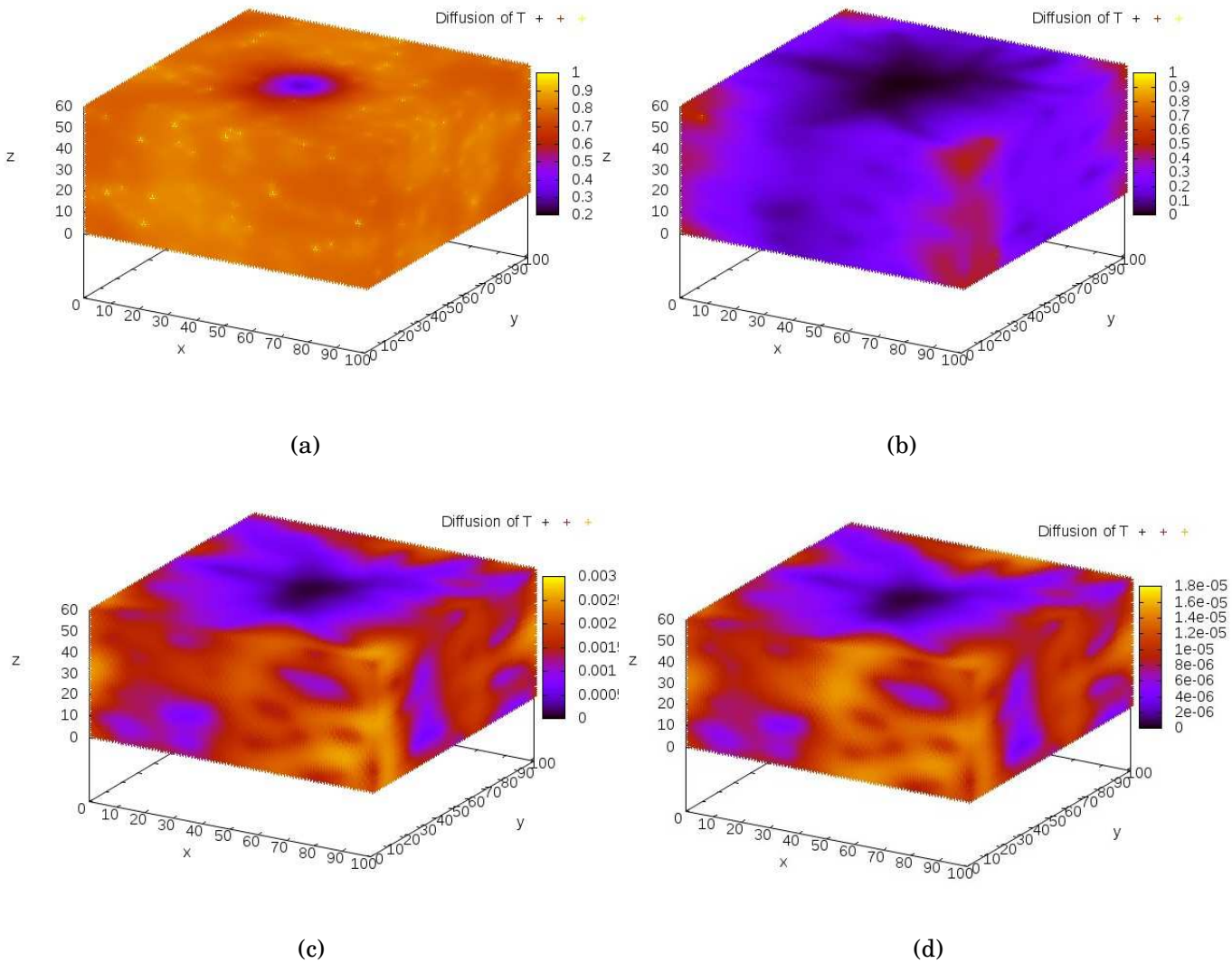

(a) (b)

(c) (d)

Figure 4.13: Parameter T for (a) 5000; (b) 25000; (c) 35000; (d) 45000 iterations, for $\alpha_P = 2.0$. Higher values of proliferation rate lead to a distribution of the parameter T with lower values comparing to a lower value of proliferation rate.

The values of T in the scales of the previous figures are consistent with what was expected.

In particular, the fast growth of the vascular tree for $\alpha = 2.0$ leads to a faster depletion of T, dropping to almost zero in 35000 iterations.

The files $alphaT1.0t.gif$ and $alphaT2.0t.gif$ in the attached CD are the videos of the time evolution of the values of T for $\alpha_P = 1.0$ and $\alpha_P = 2.0$, respectively, from 5000 to 45000 temporal iterations.

4.4 Analysis of the effect of the chemotactic response χ on the system dynamics

In this stage of the work, we decided to use a value of $T_c = 0.2$, in order to decrease the number of ramifications and being easier to compare the results. This value is still lower than the maximum value for T_c calculated in Appendix A.

Using this value of T_c and in order to compare and analyse the effect of the chemotactic response χ on the system dynamics, two values of the chemotactic response were used in the simulation. The values $\chi = 500$ and $\chi = 1000$ were used.

This parameter influences the magnitude of the vessels response to the existence of angiogenic factor. It is the parameter which influences the velocity at which tip cells move along the system. Since χ is proportional to the velocity of tip cells, higher values of χ will lead to thinner and more ramified vessels. The reason for being thinner lies in the fact that, as the velocity is higher, every cell stays a smaller period of time in every point of the system, being unable to proliferate more. This fact leads, obviously, to the occurence of thinner vessels. The increase in the number of ramifications may be explained by the fact that, being thinner, more empty spaces are left between ramifications that allow the emergence of new tip cells and, consequently, new vessels.

The parameters used in the following figures were:

- $d = 20$
- $\alpha_P = 1.0$
- $N = 1000$

The following figures show the evolution of the parameter ϕ for both the considered χ values and for 5000, 10000, 15000, 20000, 25000 and 30000 temporal iterations.

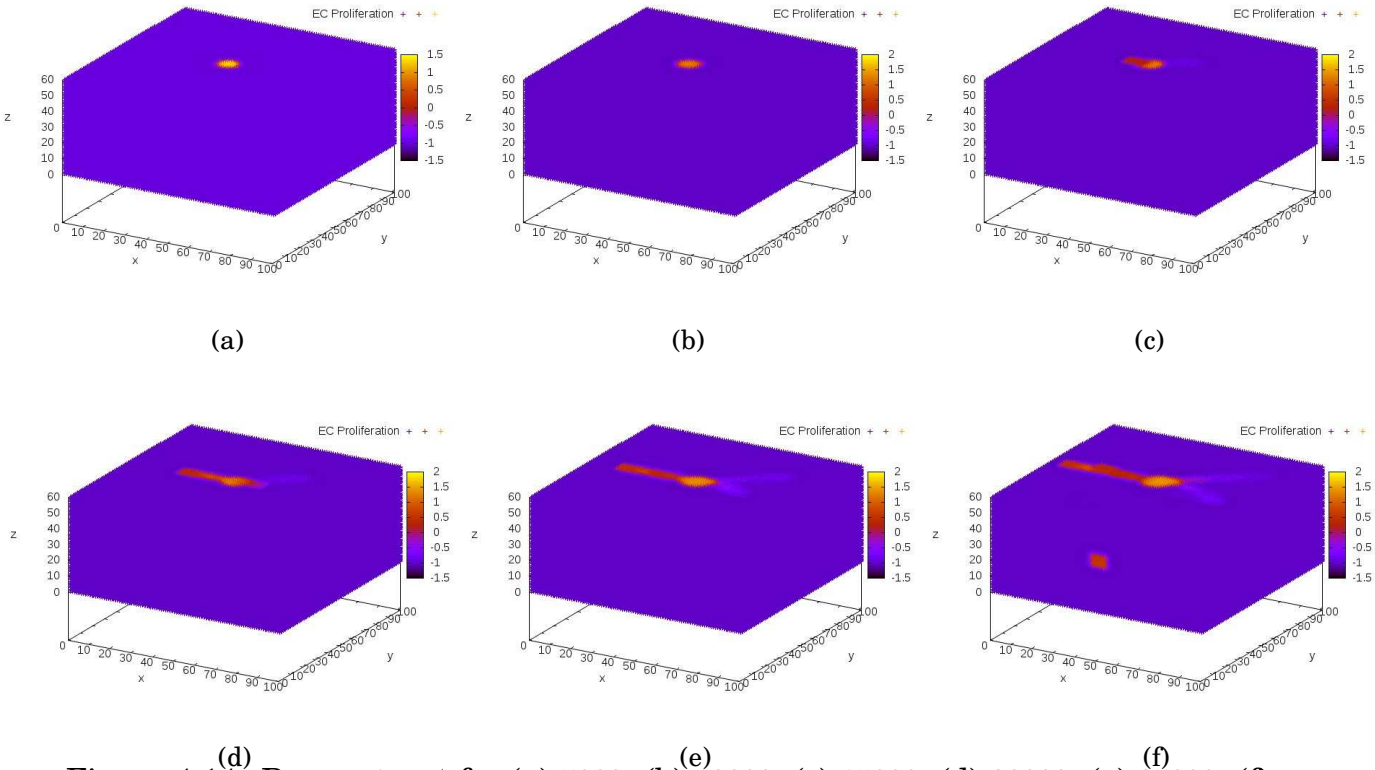

Figure 4.14: Parameter ϕ for (a) 5000; (b) 10000; (c) 15000; (d) 20000; (e) 25000; (f) 30000 iterations, for $\chi = 500$. Lower values of chemotactic response lead to thicker and less ramified vessels.

In figures 4.14 and 4.15, it appears that for $\chi = 1000$ the vessels are thinner and more ramified than for $\chi = 500$.

In order to better verify this aspect, the tree-like figures were obtained.

Figures 4.16 and 4.17 show the points with $\phi > 0$, points where there is capillar for both the considered χ values and for 5000, 10000, 15000, 20000, 25000 and 30000 temporal iterations.

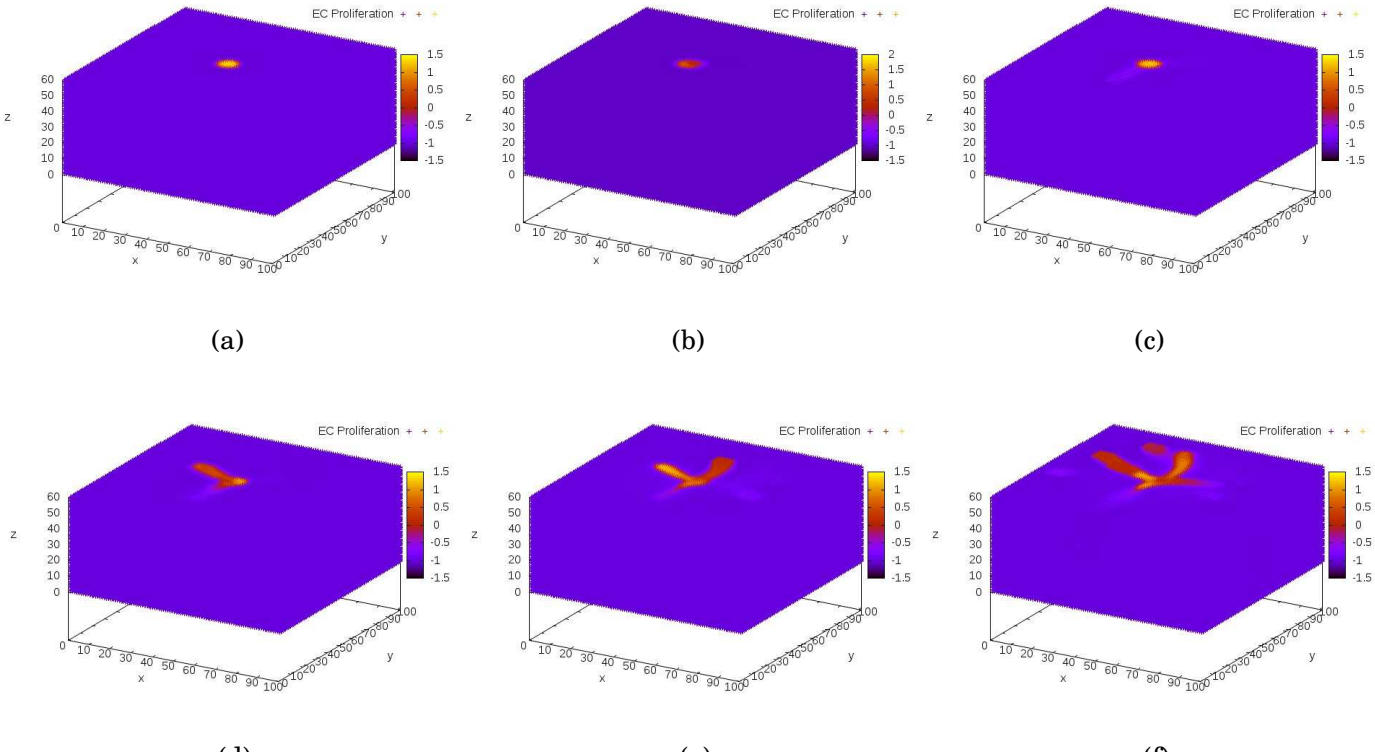

(a) (b) (c)

(d) (e) (f)

Figure 4.15: Parameter ϕ for (a) 5000; (b) 10000; (c) 15000; (d) 20000; (e) 25000; (f) 30000 iterations, for $\chi = 1000$. Higher values of chemotactic response lead to thinner and more ramified vessels.

The number of ramifications becomes clearer in figures 4.16 and 4.17. Because there are many vessels in these two structures, in this 3D representations, though we are left with the impression of thinner vessels, we cannot be certain. However, because of the lower value of χ, the network for $\chi = 500$ grows slower than for $\chi = 1000$, and if it was left to evolve for a longer time (to reach the size of the $\chi = 1000$ network at 30000 iterations), we expect the vessels to become much thicker. In any case, the introduction of a function in the simulation that would allow the achievement of a numerical analysis of the width of the vessels and of the number of branches as well, would be very useful. This is one of the aspects which would be important to introduce in the future in order to improve the analysis of the obtained results.

The files $chi500phi.gif$, $chi1000phi.gif$, $chi500phitree.gif$, $chi1000phitree.gif$ in the attached CD are the videos of the time evolution of the values of ϕ for $\chi = 500$ and $\chi = 1000$, and the tree-like figures for both the χ values, respectively.

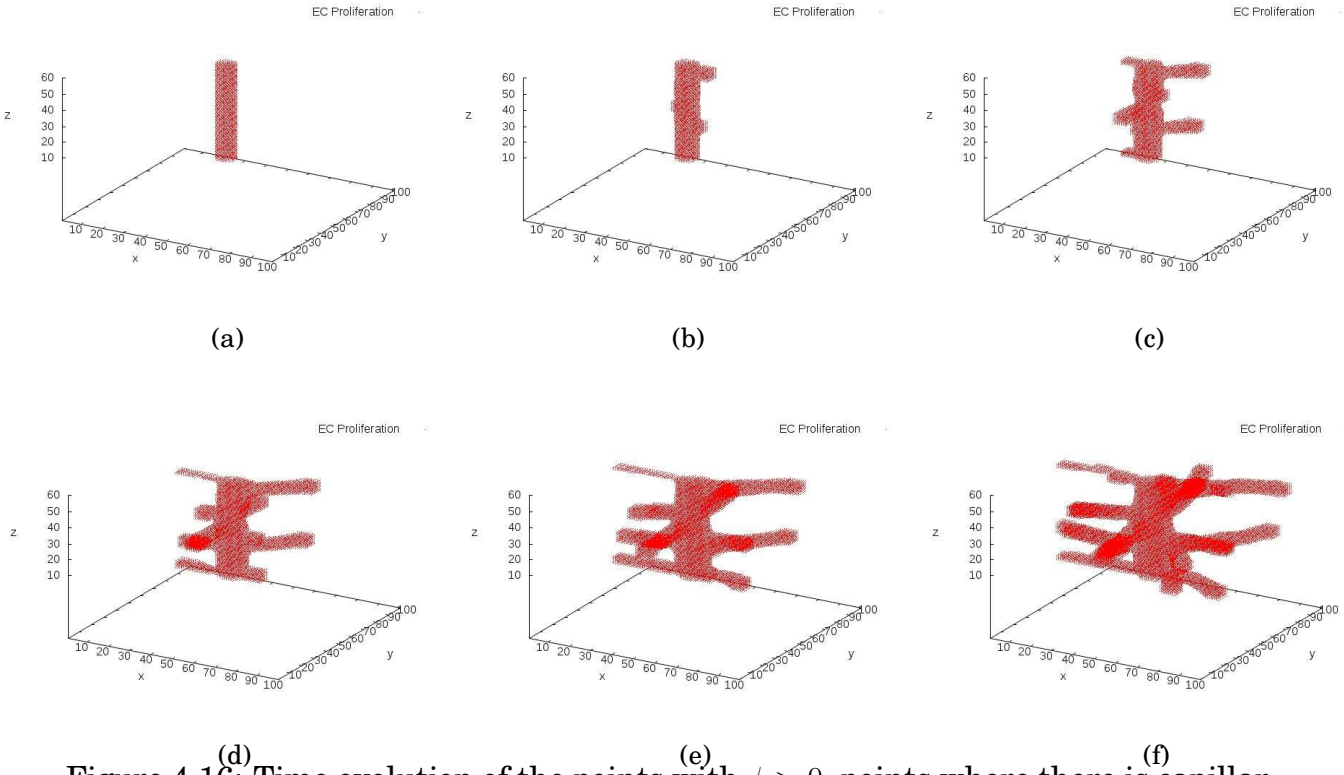

(a) (b) (c)

(d) (e) (f)

Figure 4.16: Time evolution of the points with $\phi > 0$, points where there is capillar for (a) 5000; (b) 10000; (c) 15000; (d) 20000; (e) 25000; (f) 30000 iterations, for $\chi = 500$. Lower values of chemotactic response lead to thicker and less ramified vessels.

Figures 4.18 and 4.19 show the time evolution of factor T for both χ values. Trees with thicker vessels are expected to lead to a higher consumption of angiogenic factor.

The angiogenic factor consumption is similar in the two cases studied since, while the vessels with $\chi = 500$ are expectedly thicker, the vessels with $\chi = 1000$ are more ramified. These two aspects contribute to angiogenic factor consumption.

The files $chi500t.gif$ and $chi1000t.gif$ in the attached CD are the videos of the time evolution of the values of T for $\chi = 500$ and $\chi = 1000$, respectively.

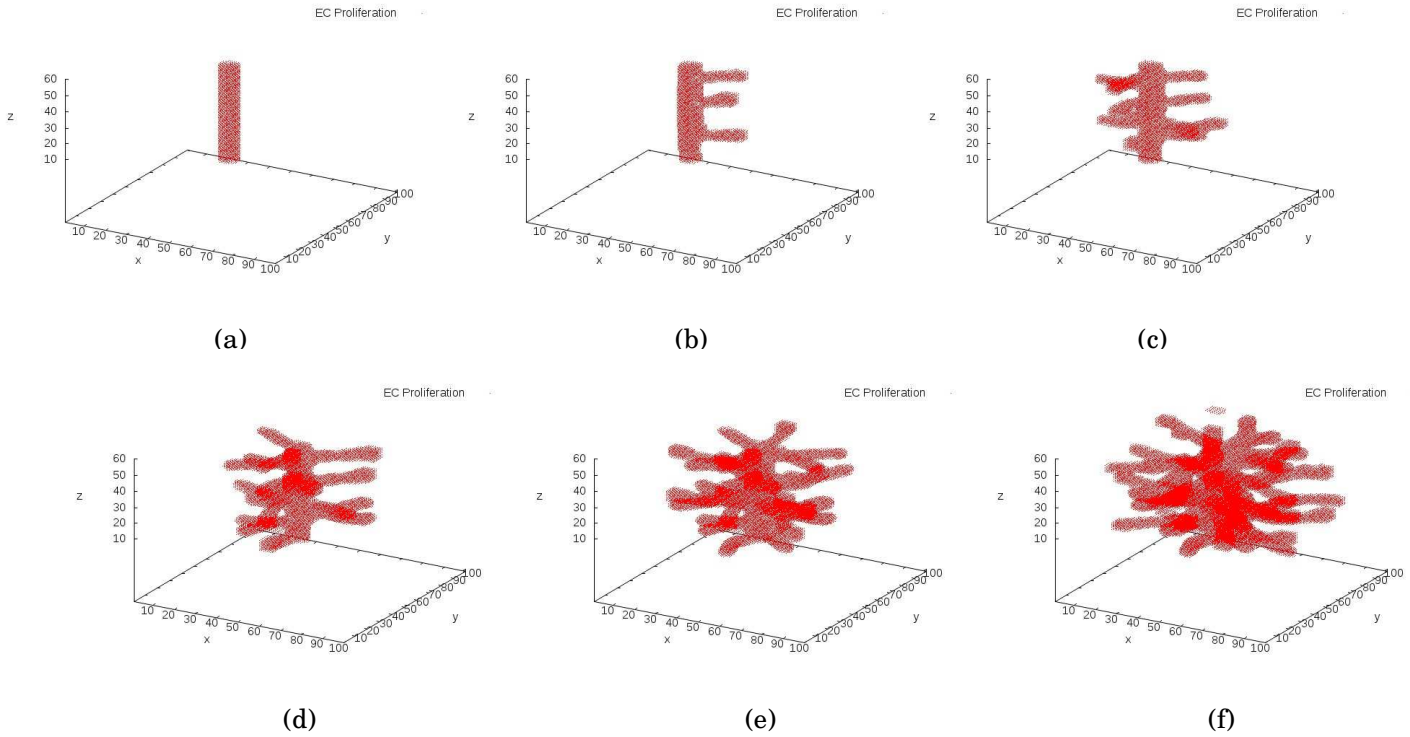

Figure 4.17: Time evolution of the points with $\phi > 0$, points where there is capillar for (a) 5000; (b) 10000; (c) 15000; (d) 20000; (e) 25000; (f) 30000 iterations; for $\chi = 1000$. Higher values of chemotactic response lead to thinner and more ramified vessels.

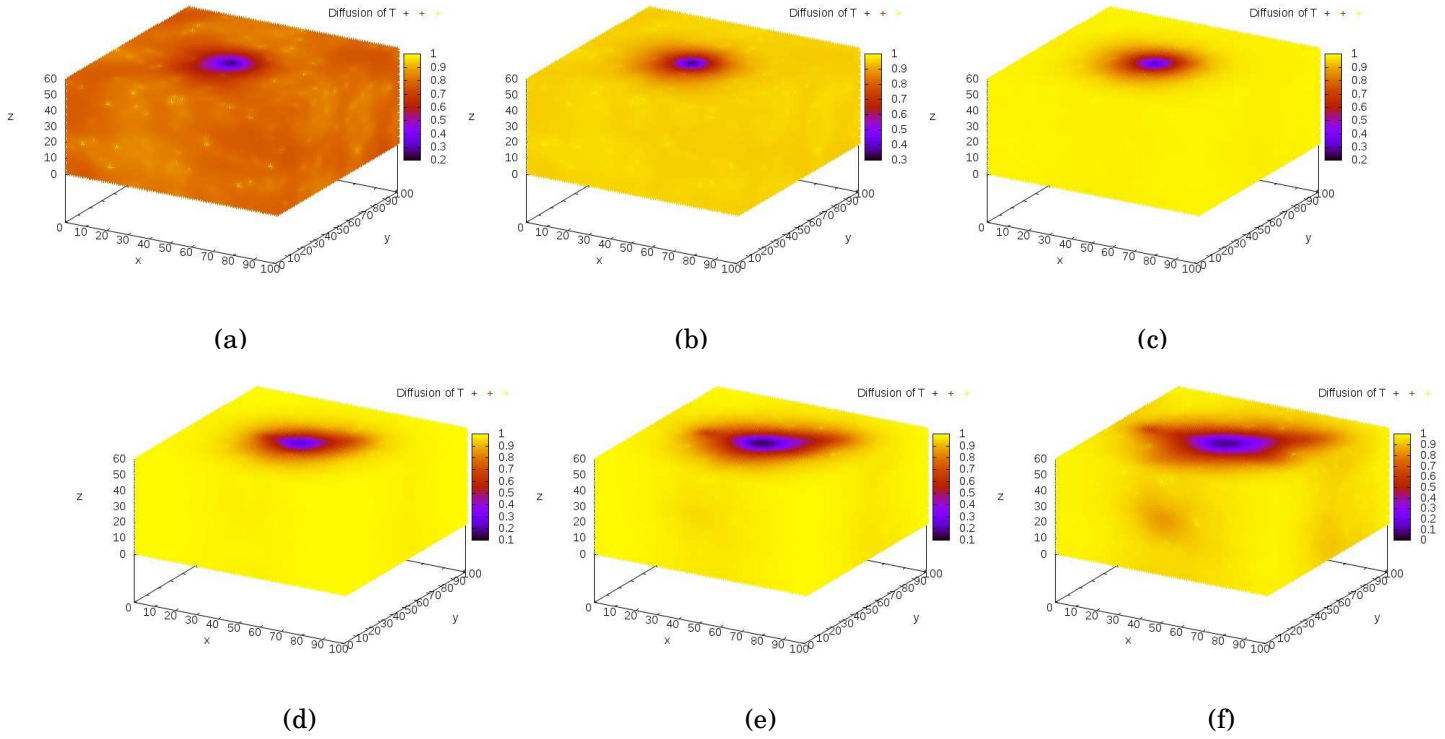

Figure 4.18: Parameter T, for (a) 5000; (b) 10000; (c) 15000; (d) 20000; (e) 25000; (f) 30000 iterations; for $\chi = 500$.

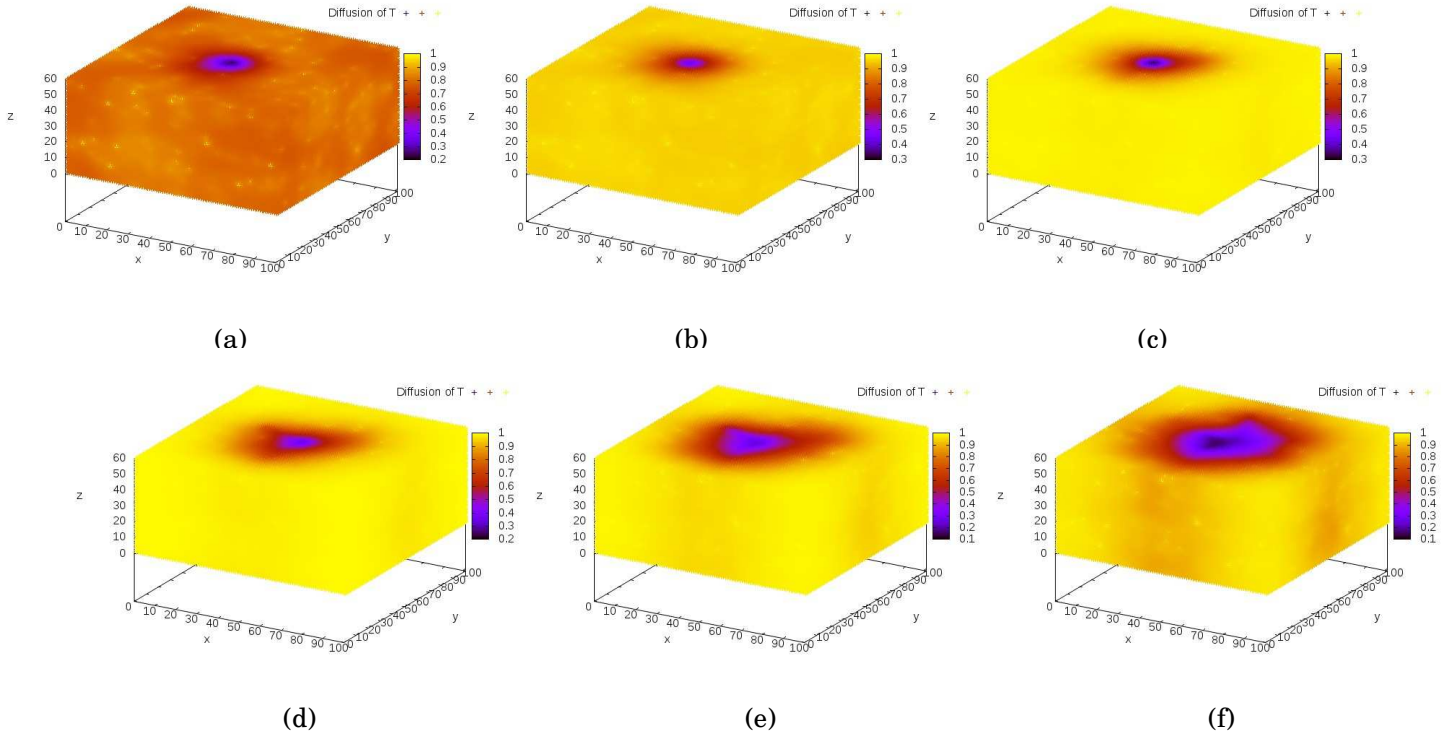

Figure 4.19: Parameter T, for (a) 5000; (b) 10000; (c) 15000; (d) 20000; (e) 25000; (f) 30000 iterations; for $\chi = 1000$.

Chapter 5

Conclusions and Future Work

Angiogenesis is a complex process that involves a large amount of proteins and factors which must be thoroughly controled, allowing an adequate stimulus to occur. However, this not always happens and in the last 20 years, angiogenesis has been seen by investigators of various fields as a way to obtain promising therapeutics that would improve the life of at least 1 bilion of people worldwide.

The central goal of this project was achieved with success. The model is now completely implemented in 3D.

The program was tested for various different parameters. The number of hypoxic cells introduced in the system, the chemotactic response of tip cells and the proliferation rate of stalk cells were changed to different values and the results obtained analysed. From this analysis, it became clear that the implementation of the model was successful since all of the results agree with the aspects theoretically and mathematically expected.

The fact of being a three-dimensional simulation is an inovative aspect of this simulation since there are very few models of angiogenesis in 3D, leading the study and results to more realistic versions of the process of angiogenesis.

Nevertheless, it would be interesting to include in the model and in the simulation some other aspects considered in other models studied in order to improve the results and obtain a better approximation to the reality.

One of these aspects is the differentiation of the various VEGF isoforms in the equation that modulates the balance between angiogenic factors, and also consider their heparin-binding properties which would affect their velocity and travelled distance during their diffusion.

Some other aspects could be included in the model such as the hapto-taxis stimulus, the angipoietins regulation action and the HIF stimulus. The EM could also be considered a viscoelastic fluid and not only the diffusion medium.

One of the future steps of this project is to parallelize the program, using the cluster milipeia. The classes of Parallel Computation were an essential background for the achievement of this future goal.

Once the program includes the most important aspects of angiogenesis and is fully optimized, its application to pathological conditions would be a very interesting step. Cancer and Diabetic Retinopathy are two disorders which, due to the incidence in the world's population, would be important to simulate.

Appendix A

Deduction of the expressions of T_c and α_T

The expression for T_c, the angiogenic factor concentration for branching, is estimated finding the steady state solution for T in 2D, continuous at $r = a$, the radius of the initial capillary, and considering that $T = 1$ at $r = d + a$, the nearest position of the sources of angiogenic factor in the tissue.

Simplifying equation 3.1 for a very sharp interface, the following equations are obtained in 2D:

$$\partial_t T = D\nabla^2 T, x \geq 0 \tag{A.1}$$

and

$$\partial_t T = D\nabla^2 T - \alpha_T T, x < 0. \tag{A.2}$$

In polar coordinates, the previous equations become:

$$D\nabla^2 T = 0 \Leftrightarrow \frac{D}{r}\partial_r(r\partial_r T) = 0 \Leftrightarrow r\partial_r T = c_1 \Leftrightarrow \tag{A.3}$$

$$\Leftrightarrow \partial_r T = \frac{c_1}{r} \Leftrightarrow T = c_1 \ln(r) + c_2$$

and

$$D\nabla^2 T - \alpha_T T = 0 \Leftrightarrow \frac{D}{r}\partial_r(r\partial_r T) - \alpha_T T = 0 \Leftrightarrow \tag{A.4}$$

$$\Leftrightarrow \partial_r T + r\partial_r^2 T - \frac{\alpha_T r}{D}T = 0 \Leftrightarrow r^2\partial_r^2 T + r\partial_r T - \frac{\alpha_T}{D}r^2 T = 0.$$

Substituing the expression $\sqrt{(\frac{\alpha_T}{D})}r$ by x, we have:

$$x^2\partial_x^2 T + x\partial_x T - x^2 T = 0. \tag{A.5}$$

The solution to the previous equation using the bessel functions I_0 and K_0 is:

$$T = c_3 I_0(x) + c_4 K_0(x) \tag{A.6}$$

and since the shape of the curve that defines the evolution of T in the space is an exponential with a positive exponent, the second term of the right side of the previous equation is ignored. The final expression for T is the following:

$$T = c_3 I_0(\frac{r}{R_c}). \tag{A.7}$$

Three conditions are used to find the three constants c_1, c_2 and c_3 of the equations A.3 and A.7:

- The value of T in the nearest source to the capillar is 1; $T(a+d) = 1$
- T must be continuous at a
- The derivative of T must be continuous at a

The three conditions referred can be transformed in an equations system, as follows:

$$\begin{cases} c_1 \ln(a+d) + c_2 = 1 \\ c_1 \ln(a) + c_2 = c_3 I_0(\frac{a}{R_c}) \\ \frac{c_1}{a} = c_3 \frac{I_{-1}(\frac{a}{R_c})}{R_c} \end{cases} \Leftrightarrow \begin{cases} c_1 = \frac{xI_{-1}(x)}{I_0(x) + xI_{-1}(x)\ln(\frac{a+d}{a})} \\ c_2 = \frac{I_0(x) - xI_{-1}(x)\ln(a)}{I_0(x) + xI_{-1}(x)\ln(\frac{a+d}{a})} \\ c_3 = \frac{1}{I_0(x) + xI_{-1}(x)\ln(\frac{a+d}{a})} \end{cases}$$

where $x = \frac{a}{R_c}$

At a distance of R_c inside the capillar, the value of T that allows the occurence of branching is T_c, which can be calculated by finding the value of $T(a - R_c)$.

$$T(a-R_c) = \frac{I_0(\frac{a-R_c}{R_c})}{I_0(x) + xI_{-1}\ln(\frac{a+d}{a})} \Leftrightarrow T(a-R_c) = \frac{I_0(\frac{a}{R_c} - 1)}{I_0(\frac{a}{R_c}) + \frac{a}{R_c} I_{-1}(\frac{a}{R_c})\ln(1 + \frac{d}{a})} \tag{A.8}$$

The value of a is the radius of the capillar (cell radius=5, in this simulation).

For the values in the simulation we obtain that $T(a - R_c) \approx 0.34$, which means that the parameter T_c should be smaller than 0.34 for branching to occur.

Appendix B

Deduction of the Equation 3.1 [1, 2, 3]

Equation 3.1 describes the evolution of the factor T, the balance between the angiogenic factors intervening in the process of angiogenesis.

The continuity equation states that a change in the density in any part of a system is due to inflow or outflow of material into or out of the system and its expression is the following:

$$\frac{\partial T}{\partial t} + \nabla \cdot \vec{j} = 0, \tag{B.1}$$

where $\vec{j}$ is the flux of the diffusing material.

Considering the expression of the first Fick's law in three dimensions:

$$\vec{J} = -D\,\nabla T(\vec{r}, t) \tag{B.2}$$

and replacing the flux $\vec{J}$ in the continuity equation, the equation becomes as follows:

$$\frac{\partial T}{\partial t} + \nabla \cdot (-D \nabla T(\vec{r}, t)) = 0. \tag{B.3}$$

Since D, the diffusion constant is not a function but a constant value, D may be withdrawn out of the brackets and the divergence of the previous equation will be performed on the gradient of T, which results in the laplacian of T, as expressed by the following equation:

$$\frac{\partial T}{\partial t} - D\,\nabla^2 T = 0 \leftrightarrow \frac{\partial T}{\partial t} = D\,\nabla^2 T. \tag{B.4}$$

Equation 3.2 is completed, adding to equation A.4 the term of consumption of angiogenic factors.
In this term, appears the consumption rate α_T, the values of T and ϕ and the Heaviside function. Because of this function, the consumption term is only present inside the capillar where the angiogenic factors are consumed by the ECs that compose it and, on the outside of the capillar, the angiogenic factors only diffuse from its production sites, the randomly distributed hypoxic cells.

Appendix C

Deduction of the Equation 3.2 [1, 2, 3]

In what concerns equation 3.2, ϕ represents an order parameter which is distributed in the system. To this distribution, a free energy is associated given by $F[\phi]$, with F the free energy of the system, a functional depending on ϕ, the phase-field variable of the model.

In this model, the authors consider the existence of two phases of ϕ in the system, one representing the capillar's interior and the other its exterior, separated by an interface. Inside the capillar, $\phi = 1$ and outside $\phi = -1$ and, consequently, the capillar wall is defined by $\phi = 0$.

The Ginzburg-Landau free energy functional is given by:

$$F[\phi] = \int \left[f(\phi) - \frac{\epsilon}{2} (\nabla\phi)^2 \right] dr, \tag{C.1}$$

where $f(\phi)$ is a function of ϕ defined by:

$$f(\phi) = -\frac{\phi^2}{2} + \frac{\phi^4}{4}. \tag{C.2}$$

The values assumed by the function f that minimize the free energy will be the minimal values of f. Solving $\frac{df}{d\phi} = 0$ gives:

$$\phi = -1 \vee \phi = 1 \vee \phi = 0. \tag{C.3}$$

The two minimal values $\phi = -1$ and $\phi = 1$ correspond to the two equilibrium stages, the two phases of ϕ in the system. $\phi = 0$ corresponds to the place represented by the interface and the term $\frac{\epsilon}{2} (\nabla\phi)^2$ arises as a 'penalty' term from the extra energetic cost associated with the transition region between the two phases. ϵ represents the interface width of the capillaries. When the order parameter ϕ is not conserved, an appropriate equation for the time evolution of the field ϕ is:

$$\frac{\partial\phi}{\partial t} = -\frac{\delta F}{\delta\phi}, \tag{C.4}$$

where the minus sign is due to the system evolution towards the minimization of the free energy.

For the conserved case, the quotient $\frac{\partial \phi}{\partial t}$ is written as:

$$\frac{\partial \phi}{\partial t} + \nabla \cdot \vec{j} = 0, \tag{C.5}$$

which is the continuity equation, where $\nabla \cdot \vec{j}$ is the divergence of $\vec{j}$, and $\vec{j}$ is given by:

$$\vec{j} = M(-\nabla \mu) \tag{C.6}$$

and μ is the chemical potential given by:

$$\mu = \frac{\delta F[\phi]}{\delta \phi}. \tag{C.7}$$

The time evolution of the order parameter ϕ, depends also on a constant M which represents the ECs' mobility; consequently, we have:

$$\frac{\partial \phi}{\partial t} = M\,(-\nabla^2 \frac{\delta F}{\delta \phi}). \tag{C.8}$$

From the definition of functional derivative, we have:

$$F[\phi + \delta\phi] - F[\phi] = \int \frac{\delta F}{\delta \phi} \delta\phi \, dr. \tag{C.9}$$

To determine the expression of $\frac{\delta F}{\delta \phi}$, the expression of $F[\phi + \delta\phi] - F[\phi]$ must be determined before.

$F[\phi + \delta\phi]$ is given by:

$$F[\phi + \delta\phi] = \int \Bigg[- \frac{(\phi + \delta\phi)^2}{2} + \frac{(\phi + \delta\phi)^4}{4} + \frac{\epsilon}{2}[\nabla\phi + \nabla\delta\phi]^2 \Bigg] dr. \tag{C.10}$$

Solving the previous equation, we obtain:

$$F[\phi + \delta\phi] = \int \Bigg[- \frac{\phi^2 + 2\phi\delta\phi + \delta\phi^2}{2} + \frac{\phi^4 + \delta\phi^4 + 2\phi^2\delta\phi^2 + 4\phi^3\delta\phi + 4\phi^2\delta\phi^2 + 4\phi\delta\phi^3}{4} + \tag{C.11}$$

$$\frac{\epsilon}{2}[(\nabla\phi)^2 + 2\nabla\phi\nabla\delta\phi + (\nabla\delta\phi)^2] \Bigg] dr,$$

which can be simplified to the following expression as the powers of $\delta\phi$ with exponent higher than 1 are negligible:

$$F[\phi + \delta\phi] = \int \Bigg[- \frac{\phi^2 + 2\phi\delta\phi}{2} + \frac{\phi^4 + 4\phi^3\delta\phi}{4} + \frac{\epsilon}{2}[(\nabla\phi)^2 + 2\nabla\phi\nabla\delta\phi] \Bigg] dr \tag{C.12}$$

$$. \tag{C.13}$$

Since $F[\phi]$ is given by:

$$F[\phi] = \int \Big[-\frac{\phi^2}{2} + \frac{\phi^4}{4} + \frac{\epsilon}{2}(\nabla\phi)^2 \Big] dr, \tag{C.14}$$

the expression of $F[\phi + \delta\phi] - F[\phi]$ is given by:

$$F[\phi + \delta\phi] - F[\phi] = \int \Big[-\phi\delta\phi + \phi^3\delta\phi + \epsilon\nabla\phi\nabla\delta\phi \Big] dr. \tag{C.15}$$

In order to find an expression putting $\delta\phi$ in evidence, the term $\epsilon\nabla\phi\nabla\delta\phi$ must be integrated once by parts. After a bit of algebra, the obtained expression to $F[\phi + \delta\phi] - F[\phi]$ is the following:

$$F[\phi + \delta\phi] - F[\phi] = \int \Big[(-\phi + \phi^3 - \epsilon\nabla^2\phi)\, \delta\, \phi \Big] dr, \tag{C.16}$$

resulting in

$$\frac{\partial\phi}{\partial t} = M\,(-\frac{\delta F}{\delta\phi}) = -M(-\phi + \phi^3 - \epsilon\nabla^2\phi). \tag{C.17}$$

From the continuity equation, we take:

$$\frac{\partial\phi}{\partial t} = -\nabla\cdot\vec{j}, \tag{C.18}$$

where replacing j and μ by the expressions C.6 and C.7, gives:

$$\frac{\partial\phi}{\partial t} = M\nabla^2\frac{\delta F}{\delta\phi} = M\nabla^2(-\phi + \phi^3 - \epsilon\nabla^2\phi). \tag{C.19}$$

The right side of equation C.19 is the first term of the second equation of the model and determines the dynamics of the interface between the capillar and what surrounds it. Equation 3.3 is completed by the endothelial cell proliferation term which is composed by the values of the function ϕ, the proliferation rate $\alpha_p(T)$ and the Heaviside function. This function takes the value 1 inside the capillar and 0 outside which leads to the conclusion that outside the capillar, the equation that represents the time evolution of the phase-field parameter ϕ becomes equal to equation C.19 and, only inside the capillar, the endothelial cell proliferation term is considered.

Appendix D

Deduction of the Equation 3.6 [1]

The material produced by the region inside the tip cells, per unit time, is equal to the proliferation rate $\alpha_p(T)$ multiplied by the volume of the tip cell, $\frac{4}{3}\pi R_c^3$. In every time unit, the cell moves with a velocity ν and travels the corresponding to its area, $\pi R_c^2|\nu|$. The resulting arterial density ϕ_c (3.6) is obtained dividing the produced material by the swept area.

Appendix E

Deduction of the expressions of the gradient and laplacian of T

According to the Taylor series:

$$T(x+\delta x, y, z) = T(x, y, z) + \delta x T'(x, y, z) + O(\delta x^2) \tag{E.1}$$

and

$$T(x-\delta x, y, z) = T(x, y, z) - \delta x T'(x, y, z) + O(\delta x^2). \tag{E.2}$$

Subtracting the two previous equations gives:

$$T(x+\delta x, y, z) - T(x-\delta x, y, z) = 2\delta x T'(x, y, z) + O(\delta x^2), \tag{E.3}$$

which gives:

$$T'(x, y, z) = \frac{T(x+\delta x, y, z) - T(x-\delta x, y, z)}{2\delta x} + O(\delta x^2). \tag{E.4}$$

The previous expression gives the equation for the gradient of T of the x component.

The gradient of a vector T which is composed by three coordinates is consequently given by:

$$\nabla T(x, y, z) = \frac{T(x+\delta x, y, z) - T(x-\delta x, y, z)}{2\delta x} + \tag{E.5}$$

$$\frac{T(x, y+\delta y, z) - T(x, y-\delta y, z)}{2\delta y} + \frac{T(x, y, z+\delta z) - T(x, y, z-\delta z)}{2\delta z}.$$

In order to deduce the laplacian expression from the Taylor series, we have:

$$T(x+\delta x, y, z) = T(x, y, z) + \delta x T'(x, y, z) + \frac{\delta x^2 T''(x, y, z)}{2!} + O(\delta x^3) \tag{E.6}$$

and

$$T(x-\delta x,y,z)=T(x,y,z)-\delta xT'(x,y,z)+\frac{\delta x^2T''(x,y,z)}{2!}+O(\delta x^3). \tag{E.7}$$

Adding the two previous equations, we have:

$$T(x+\delta x,y,z)+T(x-\delta x,y,z)=2T(x,y,z)+2\frac{\delta x^2T''(x,y,z)}{2!}+O(\delta x^3), \tag{E.8}$$

which results in:

$$T''(x,y,z)=\frac{T(x+\delta x,y,z)+T(x-\delta x,y,z)-2T(x,y,z)}{\delta x^2}+O(\delta x^3), \tag{E.9}$$

the equation for the laplacian of T of the x component.

The laplacian of a vector T for a three-dimensional system is:

$$\nabla^2T(x,y,z)=\frac{T(x+\delta x,y,z)+T(x-\delta x,y,z)-2T(x,y,z)}{\delta x^2}+ \tag{E.10}$$

$$\frac{T(x,y+\delta y,z)+T(x,y-\delta y,z)-2T(x,y,z)}{\delta y^2}+\frac{T(x,y,z+\delta z)+T(x,y,z-\delta z)-2T(x,y,z)}{\delta z^2}.$$

Appendix F

Computational Model

Program cond_init_phi.f90

```
MODULE cond_init_phi
USE global
IMPLICIT NONE
PRIVATE
 PUBLIC :: phi1

CONTAINS
SUBROUTINE phi1(a1)

REAL, DIMENSION(ifinal,jfinal,kfinal) :: a1
INTEGER :: i, j, k

open(1,file='1.out',action='write')

DO i=1,ifinal
  DO j=1,jfinal
    DO k=1,kfinal
      IF (sqrt(((i-centroi)*1.0)**2+((j-centroj)*1.0)**2)<raio) THEN
        phi(i,j,k)=1.0
        write(1,*) i,j,k
      ELSE
        phi(i,j,k)=-1.0
      END IF
    END DO
  END DO
END DO


CLOSE(UNIT=1)

END SUBROUTINE phi1
END MODULE cond_init_phi
```

Program cond_init_t.f90

```
MODULE cond_init_t
USE global
USE module_d_numpontos_factor
IMPLICIT NONE
PRIVATE
PUBLIC ::  t1

CONTAINS
SUBROUTINE t1(b1,numpontosfinal)
```

```
REAL, DIMENSION(ifinal,jfinal,kfinal) :: b1
REAL :: a,b,c, dist, r, tfinal, TT, RR,Tc,d,factor
INTEGER :: afinal, bfinal, cfinal,h, i, j, k,npn, numpontosfinal,numpontos

    CALL d_numpontos_factor(numpontos,factor)


open(2,file='2.out',action='write')
t(:,:,:)=0.0
h=1
npn=0
DO WHILE (h<=(numpontos+1))
 CALL RANDOM_NUMBER(a)
 CALL RANDOM_NUMBER(b)
 CALL RANDOM_NUMBER(c)
 afinal=a*(ifinal-1)+1
 bfinal=b*(jfinal-1)+1
 cfinal=c*(kfinal-1)+1
 t(afinal,bfinal,cfinal)=1.0
 h=h+1
 IF (sqrt(((afinal-centroi)*1.0)**2+((bfinal-centroj)*1.0)**2)<(raio+d)) THEN
  t(afinal,bfinal,cfinal)=0.0
  npn=npn+1
 END IF
END DO

numpontosfinal=numpontos-npn

DO i=1,ifinal
 DO j=1,jfinal
  DO k=1,kfinal
   IF (t(i,j,k)==1.0) THEN
    WRITE(2,*) i,j,k
   END IF
  END DO
 END DO
END DO

CLOSE(UNIT=2)
CLOSE(UNIT=9)

END SUBROUTINE t1
END MODULE cond_init_t
```

File d.txt

```
20.0
1000
0.9
```

Program global.f90

```
MODULE global
IMPLICIT NONE
SAVE

INTEGER, PARAMETER :: kfinal=60, ifinal=100, jfinal=100, centroi=50, centroj=50
REAL, DIMENSION(ifinal,jfinal,kfinal) :: phi,t
REAL, PARAMETER :: delta_t=0.0005
REAL, PARAMETER :: raio=5.0
INTEGER, PARAMETER :: delta_x=1, delta_y=1, delta_z=1
INTEGER, PARAMETER :: Rc=4, chi=1000
```

```
REAL, PARAMETER :: pi = 3.1415927
REAL :: Vx,Vy,Vz,Rx,Ry,Rz,Gx,Gy,Gz,Tc,d
REAL, PARAMETER :: Gm=0.01
DOUBLE PRECISION, DIMENSION (500,3) :: tipcellsglobal
DOUBLE PRECISION, DIMENSION (500,3) :: velocity
INTEGER :: l



COMMON tipcellsglobal, velocity, l, d, Tc

END MODULE global
```

Program global2.f90

```
MODULE global2
IMPLICIT NONE

PRIVATE
PUBLIC ::  fontes

CONTAINS
SUBROUTINE fontes(numpontosfinall,a)
INTEGER :: x,y,z,i,numpontosfinall
INTEGER, DIMENSION(numpontosfinall,3) :: a
OPEN(unit=2,file='2.out',action='read')

DO i=1,numpontosfinall
 READ (2,*) x,y,z
 a(i,:)=(/x,y,z/)
END DO


END SUBROUTINE fontes
END MODULE global2
```

Program grad.f90

```
MODULE grad
USE global
IMPLICIT NONE
CONTAINS
SUBROUTINE gradiente(nova_t,i,j,k,Gx,Gy,Gz)
REAL :: Gx,Gy,Gz
REAL, DIMENSION(:,:,:) :: nova_t
INTEGER :: i,j,k
Gx=((nova_t(mod(i+delta_x-1+ifinal,ifinal)+1,mod(j-1+jfinal,jfinal)+1,mod(k-1+kfinal,kfinal)+1))- &
(nova_t(mod(i-delta_x-1+ifinal,ifinal)+1,mod(j-1+jfinal,jfinal)+1,mod(k-1+kfinal,kfinal)+1)))/2
Gy=((nova_t(mod(i-1+ifinal,ifinal)+1,mod(j+delta_y-1+jfinal,jfinal)+1,mod(k-1+kfinal,kfinal)+1))- &
(nova_t(mod(i-1+ifinal,ifinal)+1,mod(j-delta_y-1+jfinal,jfinal)+1,mod(k-1+kfinal,kfinal)+1)))/2
Gz=((nova_t(mod(i-1+ifinal,ifinal)+1,mod(j-1+jfinal,jfinal)+1,mod(k+delta_z-1+kfinal,kfinal)+1))- &
(nova_t(mod(i-1+ifinal,ifinal)+1,mod(j-1+jfinal,jfinal)+1,mod(k-delta_z-1+kfinal,kfinal)+1)))/2

END SUBROUTINE gradiente
END MODULE grad
```

Program grad2.f90

```
MODULE grad2
USE global
IMPLICIT NONE
```

```
CONTAINS
SUBROUTINE gradiente2(nova_t,i,j,k,Gx,Gy,Gz)
REAL, DIMENSION(:,:,:) :: nova_t
INTEGER :: n
INTEGER :: i,j,k,x,y,z
REAL :: Gx,Gy,Gz
Gx=0
Gy=0
Gz=0
n=0
x=-2*Rc
DO WHILE (x<=2*Rc)
y=-2*Rc
DO WHILE (y<=2*Rc)
z=-2*Rc
DO WHILE (z<=2*Rc)
IF ((x**2+y**2+z**2) .lt. ((2*Rc)**2)) THEN
 Gx=Gx+((nova_t(mod(i+x+delta_x-1+ifinal,ifinal)+1,mod(j+y-1+jfinal,jfinal)+1,mod(k+z-1+kfinal,kfinal)+1))- &
 (nova_t(mod(i+x-delta_x-1+ifinal,ifinal)+1,mod(j+y-1+jfinal,jfinal)+1,mod(k+z-1+kfinal,kfinal)+1)))/2
 Gy=Gy+((nova_t(mod(i+x-1+ifinal,ifinal)+1,mod(j+y+delta_y-1+jfinal,jfinal)+1,mod(k+z-1+kfinal,kfinal)+1))- &
 (nova_t(mod(i+x-1+ifinal,ifinal)+1,mod(j+y-delta_y-1+jfinal,jfinal)+1,mod(k+z-1+kfinal,kfinal)+1)))/2
 Gz=Gz+((nova_t(mod(i+x-1+ifinal,ifinal)+1,mod(j+y-1+jfinal,jfinal)+1,mod(k+z+delta_z-1+kfinal,kfinal)+1))- &
 (nova_t(mod(i+x-1+ifinal,ifinal)+1,mod(j+y-1+jfinal,jfinal)+1,mod(k+z-delta_z-1+kfinal,kfinal)+1)))/2
 n=n+1
 END IF
 z=z+1
 END DO
 y=y+1
END DO
x=x+1
END DO
Gx=Gx/n
Gy=Gy/n
Gz=Gz/n

END SUBROUTINE gradiente2
END MODULE grad2
```

Program laplacian.f90

```
MODULE laplacian
USE global

CONTAINS
SUBROUTINE laplaci(a,laplaciano)
IMPLICIT NONE
REAL, DIMENSION(:,:,:) :: a
REAL, DIMENSION(:,:,:) :: laplaciano
INTEGER :: x,y,z

DO x=1,ifinal
 DO y=1,jfinal
  DO z=1,kfinal
   laplaciano(x,y,z)=((a(mod(x+delta_x-1+ifinal,ifinal)+1,y,z)+ &
a(mod(x-delta_x-1+ifinal,ifinal)+1,y,z)-2*a(mod(x-1+ifinal,ifinal)+1,y,z))/(delta_x**2))+ &
((a(x,mod(y+delta_y-1+jfinal,jfinal)+1,z)+a(x,mod(y-delta_y-1+jfinal,jfinal)+1,z)- &
2*a(x,y,z))/(delta_y**2))+((a(x,y,mod(z+delta_z-1+kfinal,kfinal)+1)+ &
a(x,y,mod(z-delta_z-1+kfinal,kfinal)+1)-2*a(x,y,z))/(delta_z**2))
  END DO
 END DO
END DO

END SUBROUTINE laplaci
END MODULE laplacian
```

Program module_d_numpontos_factor.f90

```
MODULE module_d_numpontos_factor
USE global
IMPLICIT NONE
CONTAINS
SUBROUTINE d_numpontos_factor(numpontos,factor)

INTEGER :: numpontoss,numpontos
REAL :: dd,factorr,factor


open(9,file='d.txt',action='read')
 READ (9,*) dd, numpontoss, factorr
 d=dd
 numpontos=numpontoss
 factor=factorr

Tc=factor/((exp(1.0))*(1.0+(d/Rc)))
Tc=0.055

END SUBROUTINE d_numpontos_factor
END MODULE module_d_numpontos_factor
```

Program out_writer_fontes.f90

```
MODULE out_writer_fontes
 IMPLICIT NONE
 PRIVATE
 PUBLIC ::  output_writer_fontes
CONTAINS

SUBROUTINE output_writer_fontes(nova_t,ifinal,jfinal,kfinal,file_name)
 INTEGER, INTENT(IN) :: kfinal,ifinal, jfinal
 REAL, DIMENSION(ifinal,jfinal,kfinal) :: nova_t
 CHARACTER(LEN=*), OPTIONAL :: file_name
 INTEGER :: i,j,k
 CHARACTER(LEN=3) :: a


 IF (present(file_name)) THEN
  OPEN(UNIT=1, FILE='Fontes/'//file_name//'.txt', ACTION='write')
 ELSE
  OPEN(UNIT=2, FILE='files2.txt', ACTION='read')
  READ(UNIT=2, FMT=*) a

  OPEN(UNIT=1, FILE='Fontes/'//trim(a)//'.txt', ACTION='write')
 END IF

DO i=1, ifinal
 DO j=1,jfinal
  DO k=1,kfinal
   IF (nova_t(i,j,k) .eq. 1.0) THEN
    WRITE(1,*) i, j, k
   END IF
  END DO
 END DO
 WRITE(1,*) ''
```

```
END DO

CLOSE(UNIT=1)



END SUBROUTINE output_writer_fontes
END MODULE out_writer_fontes
```

Program out_writer_phi.f90

```
MODULE out_writer_phi
 IMPLICIT NONE
PRIVATE
PUBLIC ::  output_writer_phi

CONTAINS

SUBROUTINE output_writer_phi(grelha_,ifinal,jfinal,kfinal,file_name)
 INTEGER, INTENT(IN) :: kfinal,ifinal, jfinal
 REAL, DIMENSION(ifinal,jfinal,kfinal) :: grelha_
 CHARACTER(LEN=*), OPTIONAL :: file_name
 INTEGER :: i,j,k
 CHARACTER(LEN=3) :: a



IF (present(file_name)) THEN
 OPEN(UNIT=1, FILE='Phi'//file_name//'.txt', ACTION='write')
ELSE
 OPEN(UNIT=2, FILE='files1.txt', ACTION='read')
 READ(UNIT=2, FMT=*) a

 OPEN(UNIT=1, FILE='Phi'//trim(a)//'.txt', ACTION='write')
END IF


DO i=1, ifinal
 DO j=1,jfinal
  DO k=1,kfinal
   WRITE(1,*) i, j, k, grelha_(i,j,k)
  END DO
 END DO
 WRITE(1,*) ''
END DO

CLOSE(UNIT=1)



END SUBROUTINE output_writer_phi
END MODULE out_writer_phi
```

Program out_writer_t.f90

```
MODULE out_writer_t
 IMPLICIT NONE
 PRIVATE
 PUBLIC ::  output_writer_t

CONTAINS

SUBROUTINE output_writer_t(grelha_,ifinal,jfinal,kfinal,file_name)
```

```
 INTEGER, INTENT(IN) :: kfinal,ifinal, jfinal
 REAL, DIMENSION(ifinal,jfinal,kfinal) :: grelha_
 CHARACTER(LEN=*), OPTIONAL :: file_name
 INTEGER :: i,j,k
 CHARACTER(LEN=3) :: a



IF (present(file_name)) THEN
 OPEN(UNIT=1, FILE='T/'//file_name//'.txt', ACTION='write')
ELSE
 OPEN(UNIT=2, FILE='files.txt', ACTION='read')
 READ(UNIT=2, FMT=*) a

 OPEN(UNIT=1, FILE='T/'//trim(a)//'.txt', ACTION='write')
END IF


DO i=1, ifinal
 DO j=1,jfinal
  DO k=1,kfinal
   WRITE(1,*) i, j, k, grelha_(i,j,k)
  END DO
 END DO
 WRITE(1,*) ''
END DO

CLOSE(UNIT=1)



END SUBROUTINE output_writer_t
END MODULE out_writer_t
```

Program projecto.f90

```
PROGRAM projecto
USE global
USE module_d_numpontos_factor
USE cond_init_phi
USE cond_init_t
USE global2
USE laplacian
USE update
USE tip
USE SubPosicao
USE out_writer_phi
USE out_writer_t
USE out_writer_fontes

IMPLICIT NONE
REAL, DIMENSION(ifinal,jfinal,kfinal) :: nova_t, nova_phi
INTEGER :: tempo, passos,i,j,k,numpontosfinall,x,y,z,q,di2,ii,a,iii,lig,f
INTEGER, DIMENSION(1000,3) :: fonte
INTEGER :: ligado(1000)
INTEGER :: istri

CHARACTER(LEN=4) :: stri


OPEN(3,FILE='3.out',ACTION='write')
OPEN(4,FILE='4.out',ACTION='write')
OPEN(5,FILE='5.out',ACTION='write')
OPEN(7,FILE='7.out',ACTION='write')


passos=int(500.0/delta_t)
```

```
CALL phi1(phi)
CALL t1(t,numpontosfinall)
CALL fontes(numpontosfinall,fonte)


nova_t(:,:,:)=t(:,:,:)
nova_phi(:,:,:)=phi(:,:,:)

DO di2=1,500
 tipcellsglobal(di2,:)=(/0,0,0/)
 velocity(di2,:)=(/0,0,0/)
END DO


l=0
DO lig=1,numpontosfinall
 ligado(lig)=1
END DO


DO tempo=1,passos
 CALL subupdate(nova_t,nova_phi,fonte,numpontosfinall,ligado)
 IF ( MOD(tempo,5) == 0) then
  CALL tipcell(nova_phi,nova_t)
 END IF
 iii=1
 DO WHILE (iii<=l)
  CALL posicao(iii,nova_t,Rx,Ry,Rz)
  iii=iii+1
 END DO
 IF ( MOD(tempo,5000) == 0) then
  WRITE(stri,'(i4)') tempo/5000
  istri=1
  DO WHILE ( istri<=LEN(stri))
   IF (stri(istri:istri) .EQ. ' ') THEN
    stri(istri:istri)='0'
   END IF
   istri=istri+1
  END DO
  CALL output_writer_phi(nova_phi,ifinal,jfinal,kfinal,stri)
  CALL output_writer_t(nova_t,ifinal,jfinal,kfinal,stri)
  CALL output_writer_fontes(nova_t,ifinal,jfinal,kfinal,stri)
  END IF
 END DO

DO x=1,ifinal
 DO y=1,jfinal
  DO z=1,kfinal
   write(5,*) x, y, z, nova_t(x,y,z)
  END DO
 END DO
END DO

DO i=1,ifinal
 DO j=1,jfinal
  DO k=1,kfinal
   IF (nova_t(i,j,k)>Tc) THEN
    WRITE (3,*) i,j,k
   END IF
  END DO
 END DO
END DO


DO i=1,ifinal
 DO j=1,jfinal
  DO k=1,kfinal
   IF (nova_phi(i,j,k)>0.0) THEN
    WRITE (4,*) i,j,k
```

```
   END IF
  END DO
 END DO
END DO

DO i=1,ifinal
 DO j=1,jfinal
  DO k=1,kfinal
   IF (nova_t(i,j,k) .eq. 1.0) THEN
    WRITE(7,*) i,j,k
   END IF
  END DO
 END DO
END DO



CLOSE(UNIT=3)
CLOSE(UNIT=4)

OPEN(6,FILE='6.out',ACTION='write')
DO ii=1,l
 WRITE(6,*) tipcellsglobal(ii,1), tipcellsglobal(ii,2), tipcellsglobal(ii,3)
END DO

CLOSE(UNIT=6)
CLOSE(UNIT=7)

END PROGRAM projecto
```

Program SubPosicao.f90

```
MODULE SubPosicao
USE global
USE grad2
IMPLICIT NONE
CONTAINS
SUBROUTINE posicao(iii,nova_t,Rx,Ry,Rz)
REAL, DIMENSION(:,:,:) :: nova_t
INTEGER :: iii,k
REAL :: Rx,Ry,Rz
Rx=tipcellsglobal(iii,1)
Ry=tipcellsglobal(iii,2)
Rz=tipcellsglobal(iii,3)
 call gradiente2(nova_t,int(Rx),int(Ry),int(Rz),Gx,Gy,Gz)
 IF (nova_t(int(Rx),int(Ry),int(Rz)) .gt. Tc .and. sqrt(Gx**2+Gy**2+Gz**2) .gt. Gm) THEN
  Vx=chi*Gx
  Vy=chi*Gy
  Vz=chi*Gz
  Rx=Rx+delta_t*Vx
  Ry=Ry+delta_t*Vy
  Rz=Rz+delta_t*Vz
  tipcellsglobal(iii,1)=Rx
  tipcellsglobal(iii,2)=Ry
  tipcellsglobal(iii,3)=Rz
  velocity(iii,1)=Vx
  velocity(iii,2)=Vy
  velocity(iii,3)=Vz
 ELSE
 DO k=iii,l-1
  tipcellsglobal(k,1)=tipcellsglobal(k+1,1)
  tipcellsglobal(k,2)=tipcellsglobal(k+1,2)
  tipcellsglobal(k,3)=tipcellsglobal(k+1,3)
 END DO
 l=l-1
 iii=iii-1
END IF

END SUBROUTINE posicao
```

```
END MODULE SubPosicao
```

Program tip.f90

```
MODULE tip
USE global
USE grad
USE module_d_numpontos_factor
IMPLICIT NONE
CONTAINS
SUBROUTINE tipcell(nova_phi,nova_t)
REAL, DIMENSION(ifinal,jfinal,kfinal) :: nova_phi, nova_t
INTEGER :: i,j,k,x,y,z,f,ptfinal,xmin,xmax,ymin,ymax,zmin,zmax,verifxx,verifyy,verifzz,iii,jjj,kkk,t,di1,it,b
INTEGER, DIMENSION (500,3) :: tipcellslocal
REAL :: pt

b=1

DO i=1,ifinal
 DO j=1,jfinal
  DO k=1,kfinal
   IF (nova_phi(i,j,k)>0.9) THEN
    IF (nova_t(i,j,k)>Tc) THEN
    call gradiente(nova_t,i,j,k,Gx,Gy,Gz)
    IF (sqrt(Gx**2+Gy**2+Gz**2) .gt. Gm) THEN
     x=-Rc
     f=0
    DO WHILE (x<=Rc .and. f==0)
    y=-Rc
    DO WHILE (y<=Rc .and. f==0)
     z=-Rc
     DO WHILE (z<=Rc .and. f==0)
     IF ((x**2+y**2+z**2) .lt. (Rc**2)) THEN
     IF (nova_phi(mod(i+x-1+ifinal,ifinal)+1,mod(j+y-1+jfinal,jfinal)+1,mod(k+z-1+kfinal,kfinal)+1)<0.0) THEN
      f=1
     END IF
     END IF
     z=z+1
     END DO
      y=y+1
     END DO
     x=x+1
     END DO
      IF (f==0) THEN
       xmin=mod(i-4*Rc-1+ifinal,ifinal)+1
       xmax=mod(i+4*Rc-1+ifinal,ifinal)+1
       ymin=mod(j-4*Rc-1+jfinal,jfinal)+1
       ymax=mod(j+4*Rc-1+jfinal,jfinal)+1
       zmin=mod(k-4*Rc-1+kfinal,kfinal)+1
       zmax=mod(k+4*Rc-1+kfinal,kfinal)+1
       it=1
       DO WHILE (it<=l .and. f==0)
        verifxx=0
        verifyy=0
        verifzz=0
        iii=tipcellsglobal(it,1)
        jjj=tipcellsglobal(it,2)
        kkk=tipcellsglobal(it,3)
        IF (xmax>xmin) THEN
         IF (xmin<iii .and. iii<xmax) THEN
          verifxx=1
         END IF
        END IF
        IF (ymax>ymin) THEN
         IF (ymin<jjj .and. jjj<ymax) THEN
          verifyy=1
```

```
         END IF
        END IF
        IF (zmax>zmin) THEN
         IF (zmin<kkk .and. kkk<zmax) THEN
          verifzz=1
         END IF
        END IF
        IF (xmax<xmin) THEN
         IF (iii<xmax .or. iii>xmin) THEN
          verifxx=1
         END IF
        END IF
        IF (ymax<ymin) THEN
         IF (jjj<ymax .or. jjj>ymin) THEN
          verifyy=1
         END IF
        END IF
       IF (zmax<zmin) THEN
        IF (kkk<zmax .or. kkk>zmin) THEN
         verifzz=1
        END IF
       END IF
       IF (verifxx .eq. 1) THEN
        IF (verifyy .eq. 1) THEN
         IF (verifzz .eq. 1) THEN
          f=1
         END IF
        END IF
       END IF
       it=it+1
      END DO
      IF (f==0) THEN
       tipcellslocal(b,1)=i
       tipcellslocal(b,2)=j
       tipcellslocal(b,3)=k
       b=b+1
      END IF
     END IF
    END IF
   END IF
  END IF
 END DO
END DO
END DO

IF (b>1) THEN
 l=l+1
 CALL RANDOM_NUMBER(pt)
 ptfinal=INT(pt*(b-1))+1
 tipcellsglobal(l,:)=tipcellslocal(ptfinal,:)
END IF


END SUBROUTINE tipcell
END MODULE tip
```

Program update.f90

```
MODULE update
USE global
USE laplacian
IMPLICIT NONE
CONTAINS
SUBROUTINE subupdate(c1,c2,fonte,numpontosfinall,ligado)
REAL, DIMENSION(ifinal,jfinal,kfinal) :: c1,c2,c3
REAL, DIMENSION(ifinal,jfinal,kfinal) :: d1,d2
INTEGER ligado(500)
```

```
REAL, DIMENSION(ifinal,jfinal,kfinal) :: deltatt,deltaphi,deltaphi2, deltaphicubo
INTEGER, DIMENSION(numpontosfinall,3) :: fonte
INTEGER :: x,y,z,i,numpontosfinall,xmin,xmax,ymin,ymax,zmin,zmax,it,verifxx,verifyy,verifzz,iii,jjj,kkk,f,lig
INTEGER :: rx,ry,rz,ix,iy,iz
REAL :: alfat, Tp, alfaP, alfaP_T, D, M, E,dist,distnovo

D=100.0
alfat=6.25
M=1.0
E=1.0
Tp=0.3
alfaP=1.0
 c3(:,:,:)=c2(:,:,:)*c2(:,:,:)*c2(:,:,:)
 CALL laplaci(c1,deltatt)
 CALL laplaci(c2,deltaphi)
 CALL laplaci(c3,deltaphicubo)
 CALL laplaci(deltaphi,deltaphi2)

 d1(:,:,:)=c1(:,:,:)
 d2(:,:,:)=c2(:,:,:)

 DO x=1,ifinal
  DO y=1,jfinal
   DO z=1,kfinal
    IF (d2(x,y,z)>0.9) THEN
     DO lig=1,numpontosfinall
      IF (ligado(lig) .eq. 1) THEN
       dist=(ifinal*ifinal)*1.0
       DO ix=-1,1
        DO iy=-1,1
         DO iz=-1,1
          rx=fonte(lig,1)+ix*ifinal
          ry=fonte(lig,2)+iy*jfinal
          rz=fonte(lig,3)+iz*kfinal
          distnovo=real((x-rx)*(x-rx)+(y-ry)*(y-ry)+(z-rz)*(z-rz))
          IF (distnovo .lt. dist) THEN
           dist=distnovo
          END IF
         END DO
        END DO
       END DO
       IF (dist .lt. d) THEN
        ligado(lig)=0
       END IF
      END IF
     END DO
    END IF
   IF (d1(x,y,z)<Tp) THEN
    alfaP_T=alfaP*d1(x,y,z)
   ELSE IF (d1(x,y,z)>Tp) THEN
    alfaP_T=alfaP*Tp
   END IF

 xmin=mod(x-Rc-1+ifinal,ifinal)+1
 xmax=mod(x+Rc-1+ifinal,ifinal)+1
 ymin=mod(y-Rc-1+jfinal,jfinal)+1
 ymax=mod(y+Rc-1+jfinal,jfinal)+1
 zmin=mod(z-Rc-1+kfinal,kfinal)+1
 zmax=mod(z+Rc-1+kfinal,kfinal)+1

 it=1
 f=0
 DO WHILE (it<=l)
  verifxx=0
  verifyy=0
  verifzz=0
  iii=tipcellsglobal(it,1)
  jjj=tipcellsglobal(it,2)
  kkk=tipcellsglobal(it,3)
  IF (xmax>xmin) THEN
```

```
   IF (xmin<iii .and. iii<xmax) THEN
    verifxx=1
   END IF
  END IF
  IF (ymax>ymin) THEN
   IF (ymin<jjj .and. jjj<ymax) THEN
    verifyy=1
   END IF
  END IF
  IF (zmax>zmin) THEN
   IF (zmin<kkk .and. kkk<zmax) THEN
    verifzz=1
   END IF
  END IF
  IF (xmax<xmin) THEN
   IF (iii<xmax .or. iii>xmin) THEN
    verifxx=1
   END IF
  END IF
  IF (ymax<ymin) THEN
   IF (jjj<ymax .or. jjj>ymin) THEN
    verifyy=1
   END IF
  END IF
  IF (zmax<zmin) THEN
   IF (kkk<zmax .or. kkk>zmin) THEN
    verifzz=1
   END IF
  END IF
  IF (verifxx .eq. 1) THEN
   IF (verifyy .eq. 1) THEN
    IF (verifzz .eq. 1) THEN
     f=1
     EXIT
    END IF
   END IF
  END IF
  it=it+1
 END DO
 IF (f==0) THEN
  IF (d2(x,y,z) > 0.0) THEN
   c2(x,y,z)=d2(x,y,z)+delta_t*M*(-deltaphi(x,y,z)+deltaphicubo(x,y,z)-E*deltaphi2(x,y,z))+ &
   delta_t*alfaP_T*d2(x,y,z)
  ELSE IF (d2(x,y,z) <= 0.0) THEN
   c2(x,y,z)=d2(x,y,z)+delta_t*M*(-deltaphi(x,y,z)+deltaphicubo(x,y,z)-E*deltaphi2(x,y,z))
  END IF
  IF (d2(x,y,z) > 0.0) THEN
   c1(x,y,z)=d1(x,y,z)+delta_t*(D*deltatt(x,y,z))-delta_t*alfat*d2(x,y,z)*d1(x,y,z)
  ELSE IF (d2(x,y,z) <= 0.0) THEN
   c1(x,y,z)=d1(x,y,z)+delta_t*(D*deltatt(x,y,z))
  END IF
 END IF
 IF (f==1) THEN
  c2(x,y,z)=((alfaP_T*Rc*4)/(3*sqrt(velocity(it,1)**2+velocity(it,2)**2+velocity(it,3)**2)))
  c1(x,y,z)=d1(x,y,z)+delta_t*(D*deltatt(x,y,z))
 END IF
END DO
END DO
END DO

i=1

DO WHILE (i<=numpontosfinall)
 IF (ligado(i) .eq. 1) THEN
  c1(fonte(i,1),fonte(i,2),fonte(i,3))=1.0
 END IF
 i=i+1
END DO

END SUBROUTINE subupdate
```

```
END MODULE update
```

Bibliography

[1] R. Travasso, E. Poiré, M. Castro, J. Rodríguez-Manzaneque, and A. Hernandez-Machado, "Tumor angiogenesis and vascular patterning: A mathematical model.," *PLoS ONE*, vol. 5, May 2011.

[2] A. Bray, "Theory of phase ordering kinetics," *Physica A: Statistical Mechanics and its Applications*, vol. 194, no. 1-4, pp. 41–52, 1993.

[3] H. Emmerich, *The diffuse interface approach in materials science: thermodynamic concepts and applications of phase-field models*. Springer, 2003.

[4] *Lecture 1: Vasculogenesis and angiogenesis. Department of Medical Biotechnology; Faculty of Biochemistry, Biophysics and Biotechnology Jagiellonian University. Poland*.

[5] T. H. Adair and J.-P. Montani, *Angiogenesis*. Morgan & Claypool Life Sciences, 2010.

[6] R. K. Jain, "Normalization of tumor vasculature: an emerging concept in antiangiogenic therapy.," *Science*, vol. 307, pp. 58–62, Jan. 2005.

[7] A. L. Bauer, T. L. Jackson, and Y. Jiang, "A cell-based model exhibiting branching and anastomosis during tumor-induced angiogenesis.," *Biophys J*, vol. 92, pp. 3105–21, May 2007.

[8] "http://www.angiopoietin.de (viewed in 21/02/2011)."

[9] M. J. Plank, B. D. Sleeman, and P. F. Jones, "A mathematical model of tumour angiogenesis, regulated by vascular endothelial growth factor and the angiopoietins.," *J Theor Biol*, vol. 229, pp. 435–54, Aug. 2004.

[10] G. M. Cooper and R. E. Hausman, *The cell: a molecular approach*. ASM press Washington, DC, 2009.

[11] M. J. Karkkainen and T. V. Petrova, "Vascular endothelial growth factor receptors in the regulation of angiogenesis and lymphangiogenesis.," *Oncogene*, vol. 19, pp. 5598–605, Nov. 2000.

[12] P. Carmeliet, "Angiogenesis in life, disease and medicine.," *Nature*, vol. 438, pp. 932–6, Dec. 2005.

[13] I. Buschmann and W. Schaper, "Arteriogenesis versus angiogenesis: Two mechanisms of vessel growth.," *News Physiol Sci*, vol. 14, pp. 121–125, June 1999.

[14] L. T. Krebs, Y. Xue, C. R. Norton, J. R. Shutter, M. Maguire, J. P. Sundberg, D. Gallahan, V. Closson, J. Kitajewski, R. Callahan, G. H. Smith, K. L. Stark, T. Gridley, *et al.*, "Notch signaling is essential for vascular morphogenesis in mice.," *Genes Dev*, vol. 14, pp. 1343–52, June 2000.

[15] "http://www.copewithcytokines.de/cope.cgi?key=angioblasts, viewed in 21/02/2011."

[16] H. Gerhardt and C. Betsholtz, "Endothelial-pericyte interactions in angiogenesis.," *Cell Tissue Res*, vol. 314, pp. 15–23, Oct. 2003.

[17] W. S. N. Shim, I. A. W. Ho, and P. E. H. Wong, "Angiopoietin: a tie(d) balance in tumor angiogenesis.," *Mol Cancer Res*, vol. 5, pp. 655–65, July 2007.

[18] M. Héroult, F. Schaffner, and H. G. Augustin, "Eph receptor and ephrin ligand-mediated interactions during angiogenesis and tumor progression.," *Exp Cell Res*, vol. 312, pp. 642–50, Mar. 2006.

[19] M. J. Holmes and B. D. Sleeman, "A mathematical model of tumour angiogenesis incorporating cellular traction and viscoelastic effects.," *J Theor Biol*, vol. 202, pp. 95–112, Jan. 2000.

[20] A. Shirinifard, J. S. Gens, B. L. Zaitlen, M. Swat, and J. A. Glazier, "3d multi-cell simulation of tumor growth and angiogenesis.," *PLoS One*, vol. 4, no. 10, p. e7190, 2009.

[21] M. Heil, I. Eitenmüller, T. Schmitz-Rixen, and W. Schaper, "Arteriogenesis versus angiogenesis: similarities and differences.," *J Cell Mol Med*, vol. 10, no. 1, pp. 45–55, 2006.

[22] A. Rehman and C. Wang, "Notch signaling in the regulation of tumor angiogenesis," *Trends in cell biology*, vol. 16, no. 6, pp. 293–300, 2006.

[23] "http://www.biooncology.com/index.html (viewed in 08/06/2011)."

[24] H. Gerhardt, M. Golding, M. Fruttiger, C. Ruhrberg, A. Lundkvist, A. Abramsson, M. Jeltsch, C. Mitchell, K. Alitalo, D. Shima, and C. Betsholtz, "Vegf guides angiogenic sprouting utilizing endothelial tip cell filopodia.," *J Cell Biol*, vol. 161, pp. 1163–77, June 2003.

[25] G. Melillo, "Inhibiting hypoxia-inducible factor 1 for cancer therapy.," *Mol Cancer Res*, vol. 4, pp. 601–5, Sept. 2006.

[26] J. E. Rundhaug, "Matrix metalloproteinases and angiogenesis.," *J Cell Mol Med*, vol. 9, no. 2, pp. 267–85, 2005.

[27] T. D. Gilmore, "Introduction to nf-kappab: players, pathways, perspectives.," *Oncogene*, vol. 25, pp. 6680–4, Oct. 2006.

[28] U. Fiedler, M. Scharpfenecker, S. Koidl, A. Hegen, V. Grunow, J. M. Schmidt, W. Kriz, G. Thurston, and H. G. Augustin, "The tie-2 ligand angiopoietin-2 is stored in and rapidly released upon stimulation from endothelial cell weibel-palade bodies.," *Blood*, vol. 103, pp. 4150–6, June 2004.

[29] F. Milde, M. Bergdorf, and P. Koumoutsakos, "A hybrid model for three-dimensional simulations of sprouting angiogenesis.," *Biophys J*, vol. 95, pp. 3146–60, Oct. 2008.

[30] "http://www.gene.com/gene/products/information/oncology/avastin/ (viewed in 21/02/2011)."

[31] N. V. Mantzaris, S. Webb, and H. G. Othmer, "Mathematical modeling of tumor-induced angiogenesis.," *J Math Biol*, vol. 49, pp. 111–87, Aug. 2004.

[32] C. L. Stokes and D. A. Lauffenburger, "Analysis of the roles of microvessel endothelial cell random motility and chemotaxis in angiogenesis.," *J Theor Biol*, vol. 152, pp. 377–403, Oct. 1991.

[33] M. Chaplain and A. Stuart, "A mathematical model for the diffusion of tumour angiogenesis factors into the surrounding host tissue," *J. Math. Appl. Med. Biol.*, no. 8, pp. 191–220, 1991.

[34] M. A. Chaplain, S. M. Giles, B. D. Sleeman, and R. J. Jarvis, "A mathematical analysis of a model for tumour angiogenesis.," *J Math Biol*, vol. 33, no. 7, pp. 744–70, 1995.